UNIVERSITY OF CALIFORNIA

Los Angeles

Yes Associated Protein Plays an Essential Role in the Development and Progression of Head and Neck Squamous Cell Carcinoma

A dissertation submitted in partial satisfaction of the

requirements for the degree Doctor of Philosophy

in Oral Biology

by

David H Bae

2014

ABSTRACT OF THE DISSERTATION

Yes Associated Protein Plays an Essential Role in the Development and Progression of Head and Neck Squamous Cell Carcinoma

By

David H Bae

Doctor of Philosophy in Oral Biology

University of California, Los Angeles, 2014

Professor Cun-Yu Wang, Chair

The intricate anatomy of the primary tumor, the occurrence of late-stage diagnosis, combined with the aggressive nature of head and neck squamous cell carcinoma (HNSCC) has made this disease difficult to treat. The global rate of HNSCC continues to rise, accounting up to 25% of all new cancer cases. But despite advances in treatment, the five year survival rate has remained stagnant for decades. Therefore a clearer understanding of the formation and progression of HNSCC is essential to the development of better therapeutic approaches to prevent and treat HNSCC patients. Recent studies have identified yes associated protein (YAP)

as a potential target. YAP is a highly conserved transcriptional coactivator and has been found amplified as well as its expression upregulated and active in HNSCCs. In this study we hypothesize that YAP plays a key role in the development and progression of HNSCC. Our results show that activated YAP can transform and induce epithelial to mesenchymal transition (EMT) of our immortalized but nontransformed oral keratinocyte cell line OKF6 as seen by its ability to increase proliferation, saturation density, invasion, and induce anchorage independent growth. Moreover activated YAP potently enhances tumor formation and growth *in vivo*. YAP knockdown in HNSCC cell lines corroborated our initial findings where YAP knockdown could inhibit proliferation and invasion of HNSCC. We also discovered that YAP abundance correlated with tumor stage and lymph node metastasis in human HNSCC tissue samples. More recent studies have identified YAP regulation in response to extracellular cues. Therefore we further pursued our findings to determine whether YAP could mediate HGF induced cancer characteristics. We found that YAP knockdown could inhibit HGF induced proliferation and invasion of HNSCC, and by further microarray analysis, identified new potential targets and pathways by which YAP could direct cancer development and progression. Taken together our study not only suggests that YAP may play an important role in HNSCC, but also mediate response upon HGF stimulation to provide us with greater insight into the molecular regulation of HNSCC.

Mo Kang

Ke Shuai

Sotirios Tetradis

Cun-Yu Wang, Committee Chair

University of California, Los Angeles

2014

DEDICATION

To my friends and family.

Ever constant, always there.

TABLE OF CONTENTS

LIST OF FIGURES

LIST OF TABLES

ACKNOWLEDGEMENTS

This dissertation would not be have been possible if not for the generous support and help from the many people that I have come to know throughout my graduate training. First and foremost I would like to give my sincerest gratitude to **Dr. Cun-Yu Wang** for allowing me the great privilege of being a member of his lab. I am so deeply thankful for his insight, advice, mentorship, as well as all the help that I know he gives me without my being aware throughout the PhD program. He has taught me about science as much as he has taught me of life. I will never forget and I am truly grateful. I would like to thank my committee members **Dr. Sotirios Tetradis**, **Dr. Ke Shuai**, and **Dr. Mo Kang**, for their experimental advice, insightful comments, probing questions, and guidance. It is truly a great honor to have them as my committee members, and it is with much hope that I may continually interact with them in the years to come.

My accomplishments today are all the result from the superb faculty support here at UCLA School of Dentistry. I would like to thank **Dr. Jeanne Nervina** for convincing me to pursue research. If not for her, I would not be here to venture in the pursuit of science. I would like to thank **Dr. Wen Yuan Shi** for his constant care and advice. I would like to thank **Dr. Renate Lux**, **Dr. Anahid Jewett**, **Dr. Ki-Hyuk Shin**, and **Dr. Reuben Kim** for their continuous support and care. They were always there to give me scientific advice, help me with experiments and techniques, and critique my work. They continuously make me better.

I am indebted to the support from the Division of Oral Biology and Medicine, especially the UCLA T32 Training Program. My deepest gratitude goes to **Dr. David Wong** for being such a strong advocate for research and allowing the financial support to make my research possible.

I would also like to make a special thanks to **Megan Scott** and **Pauli Nuttle** for their tremendous help throughout my PhD training.

Lastly, I would like to thank my friends and colleagues here in the School of Dentistry. **Dr. Jeffrey Kim**, **Dr. Ben Kang**, **Dr. Nini Chaichanasakul**, **Edward Meyer**, **Trent Su**, and **Kenneth Lee**. We all went through, and are continuing to go through this together. They have made my time here enjoyable and something really worth remembering. Our friendship I will continue to cherish.

Apart from the simple joys in life, I feel that the things that are most important to an individual is seldom worth doing if not overcome with great thought, patience, and perseverance. Research has been a great blessing, and is of great importance in my life. I wish that I may have the continued privilege to contribute to the sciences and expand the research frontier.

VITA

2005	B.A., Molecular Cell Biology University of California Los Angeles, California
2007	M.S., Oral Biology and Medicine UCLA School of Dentistry Los Angeles, California
2008	Student Intramural Oral Biology Seed Grant UCLA School of Dentistry Los Angeles, California
2008	NIH T32 Student Training Grant UCLA School of Dentistry Los Angeles, California
2011	School of Dentistry Research Day Poster Competition Award (1st place) UCLA School of Dentistry Los Angeles, California
2013	School of Dentistry Research Day Poster Competition Award (1st Place) UCLA School of Dentistry Los Angeles, California

CHAPTER 1

INTRODUCTION

1.1 Head and Neck Squamous Cell Carcinoma

1.1.1 Global Head and Neck Cancer Statistics

Head and neck cancer is a broad term that encompasses a range of neoplasms that occur in one anatomic region. Under this common term, head and neck cancers include, malignancies that arise from the paranasal sinuses, nasal cavity, oral cavity, pharynx, and larynx (Fig. 1-1). Furthermore almost all head and neck cancers are considered squamous cell carcinomas (SCC) as they originate from the squamous cells that line the moist epithelial surfaces inside the head and neck.

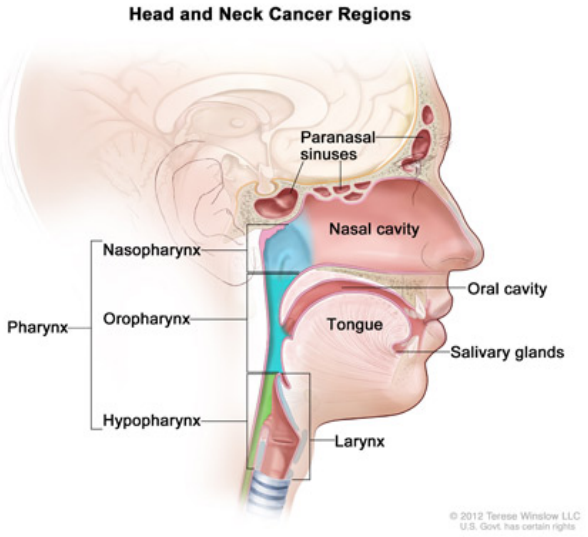

Figure 1-1. Head and neck cancer regions. Illustrates location of paranasal sinuses, nasal cavity, oral cavity, tongue, salivary glands, larynx, and pharynx (including the nasopharynx, oropharynx, and hypopharynx).
(From www.cancer.gov)

The global incidence of head and neck cancer continues to rise, making the disease an ever important public health concern. In 2008, an estimated 400,000 new head and neck cancer cases occurred globally making it the sixth most common cancer worldwide, and more than 40,000 new head and neck cancer cases arise each year in America, comprising 6% and 3% of all cancers respectively (Argiris et al. 2008; Jemal et al. 2009). Lifestyle, habits, demographics, as well as genetic factors influence geographic variations in the incidence of head and neck cancer. For example, although head and neck cancer rates in the United States may be relatively low, areas characterized by high incidence rates include South and Southeast Asia, parts of Western and Eastern Europe, and parts of Latin America and the Caribbean. In Pacific regions, head and neck cancer is the most common in men contributing up to 25% of all new cancer cases, and in the case of India, the most common cancer type accounting for 40% of all malignancies (Saman Warnakulasuriya 2009).

1.1.2 Epidemiology and Risk Factors

HNSCC is characterized by multiphasic and multifactorial etiopathogenesis. Of the causative factors so far identified, basic carcinogenic and epidemiological data have established cigarette smoke as the most important risk factor for the overwhelming majority of HNSCCs (Hashibe et al. 2006; Argiris et al. 2008). Studies have found that the risk of HNSCC for cigarette smokers is estimated to be approximately 10 fold over that of never smokers, but also that risk for ex-smokers can also decrease substantially with time since cessation showed no excess in detection among those having quit for 10 years or more (Sturgis and Cinciripini 2007; Schlecht et al. 1999). Alcohol abuse is also

associated with increased risk of HNSCC, and although cigarette smoke and alcohol consumption have been confirmed as independent risk factors for HNSCC, the use of both synergistically interacts to multiplicatively increase risk of HNSCC, attributing to at least 75% of HNSCC (Blot et al. 1988; Pelucchi et al. 2008; Hashibe et al. 2007). More recently, oral human papillomavirus (HPV) has been found to be strongly associated with HNSCC, and that HPV status is an independent prognostic factor among HNSCC patients (D'Souza et al. 2007; Gillison et al. 2008; Ang et al. 2010). In addition to the aforementioned exogenous risk factors, inherited disorders such as Fanconi anaemia, Li-Fraumeni syndrome, ataxia telangiectasia, Lynch-II syndrome, and genetic polymorphisms have been found to predispose individuals to HNSCC (Trizna and Schantz 1992; Foulkes et al. 1996; Suárez et al. 2006; Hashibe et al. 2006; Sturgis et al. 2002).

1.1.3 Recurrent and Metastatic Disease

The 20th century saw great advances in surgery, radiotherapy, and chemotherapy based approaches for treating HNSCC. In addition modern anesthesia, medications, and improved medical care has led to better patient outcome and increased quality of life. However despite these advances, the overall survival rate of HNSCC is ~50% and has not changed since the 1960's (Bose et al. 2013).

This is primarily because of the highly invasive nature of HNSCC combined with the rich lymphatic system and complexity of the head and neck region. HNSCC patients continue to die from local recurrence, second primary tumors, and metastatic disease at regional and distant sites (Sano and Myers 2007). Early detection is the most critical step

in reducing morbidity and mortality of HNSCC. About one third of patients present with stage I or stage II disease and are cured of up to 90% and 70% respectively (Argiris et al. 2008). Unfortunately, the majority of patients present with locoregionally advanced HNSCC and have a far more unfavorable prognosis with a 40%-50% 5 year overall survival (de Bree et al. 2012).

Most HNSCC patients present with cervical lymph node metastasis. As an independent prognostic factor, cervical lymph node metastasis has a great impact on the disease-free and overall survival of patients with HNSCC. Cervical metastasis is perhaps the most significant oncological factor in the prognosis of HNSCC because early detection and treatment may prevent distant metastases. Its presence drastically reduces survival rate, and in the case of squamous cell carcinoma of the oral tongue (SCCOT), can reduce the 5 year survival rate from 65% to 29%. Cervical metastasis is also closely related to the occurrence of distant metastasis in HNSCC (Leemans et al. 1993).

The incidence of distant metastasis is directly related to the clinical stage of the tumor, with higher incidence in more advanced stages, particularly in patients with advanced nodal disease. Surprisingly, distant metastases many times go undetected. Clinical detection of metastatic foci occurs from 10% to 30% of cases, whereas autopsy studies yield an incidence of approximately 50% (Leemans et al. 1993). Unfortunately, once distant metastases are detected, patients have an extremely poor prognosis. The mean survival following diagnosis of distant metastasis is 6 months and 90% of patients die within 2 years (Calhoun et al. 1994).

1.2 Epithelial to Mesenchymal Transition

1.2.1 Epithelial to Mesenchymal Transition and Metastasis

High mortality rates associated with cancer are most often caused by the metastasis, defined as the spread of cells from one primary neoplasm to the eventual growth at distant organs. Despite significant advances in diagnosis, surgical techniques, general patient care, and local and systemic adjuvant therapies, metastasis remains the cause of 90% of death from solid tumors.

Several discrete steps are discernable in the biological cascade of metastasis: loss of cellular adhesion, increased motility and invasiveness, entry and survival in the circulation, exit into new tissue, and eventual colonization at distant sites (Fig. 1-1)(Gupta and Massagué 2006). First, the metastatic tumor cell must shed its cell-cell and cell matrix interactions. Second, it must gain motility to navigate the tumor stroma, and acquire invasive capabilities allowing it to degrade the surrounding extracellular matrix and allow escape from the primary tumor mass. Third, once migrating in the hematogenous or lymphatic systems, cells must evade anoikis, cell death that is induced by the loss of adhesive support. Fourth, it must be able to extravasate, requiring adhesion capability to the distant endothelium and endothelial barrier and basement membrane penetration capability. Lastly, it must lead to the establishment and growth of micrometastasies at distant sites (Talbot et al. 2012). The first two steps are of fundamental importance, and is currently a focal topic of study where cancer cells lose their epithelial characteristics and take on properties that are more typical of mesenchymal cells in what has been termed epithelial to mesenchymal transition (EMT).

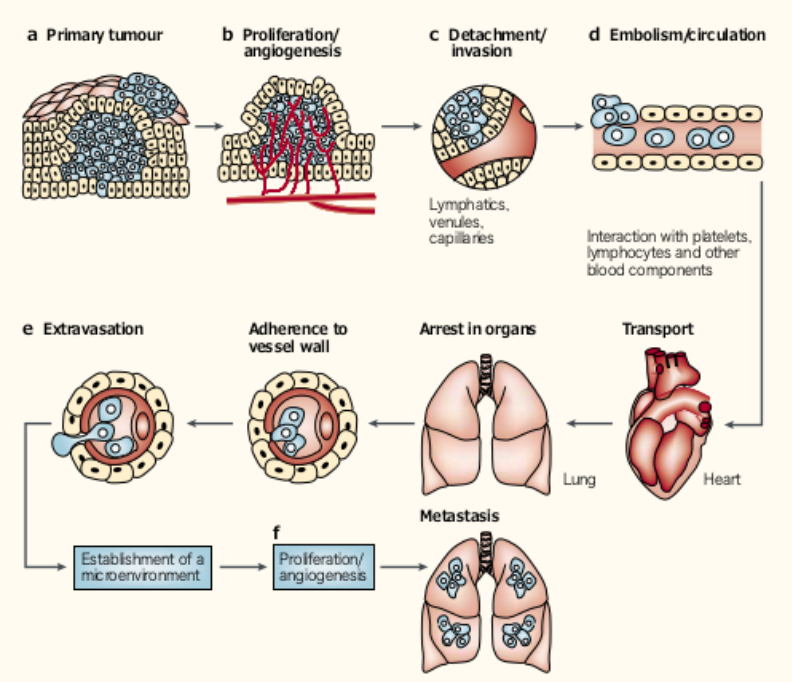

Figure 1-2. The main steps in the formation of metastasis. (a) Cellular transformation and tumor growth. (b) Extensive vascularization must occur. (c) Local invasion of the host stroma by select tumor cells. (d) Detachment and emobilization of individual tumor cells or aggregates. (e) Extravasation occurs. (f) Proliferation within the organ parenchyma completes the metastatic process. (Fidler 2003)

1.2.2 Biomarkers of EMT

EMT is considered a central event in the metastatic cascade and is the most comprehensive theory that describes how quiescent tumor cells acquire metastatic capability. The essential features of EMT are the disruption of intercellular contacts and the enhancement of cell motility, leading to the release of cells from the primary epithelial tissue. The subsequent phenotype resulting from molecular and morphological change is what allows for the progression of metastasis to occur (Huang 2008). The molecular hallmark of EMT is the downregulation of cell-cell adhesion molecule and epithelial cell molecular marker E-cadherin, and the upregulation of mesenchymal marker N-cadherin in what is referred to as cadherin switch. Upregulation of additional mesenchymal markers such as vimentin and fibronectin have also been identified to be important for EMT (Fig. 1-3).

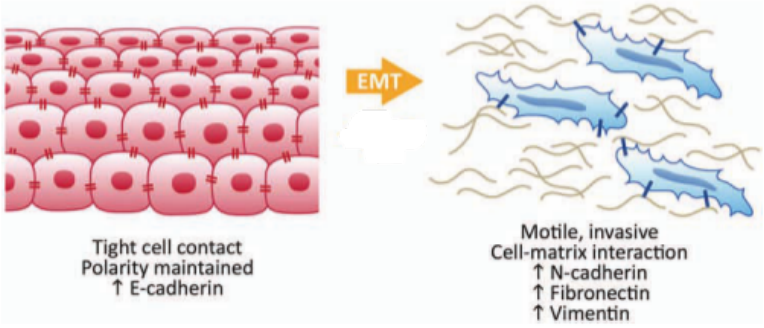

Figure 1-3. Epithelial-to-mesenchymal transition (EMT). Epithelial-like cells display tight cell-cell contacts and maintain polarity, whereas mesenchymal-like cells are more motile and display more contact with the extracellular matrix. Proteins associated with the epithelial-like or the mesenchymal-like states are referred to as biomarkers. As cells progress through EMT, levels of proteins associated with each state are altered, reflecting the phenotypic switch between the 2 states. Image adapted from (Scanlon et al. 2013).

More specifically E-cadherins are transmembrane proteins of adherens junctions that anchor epithelial cells to each other and create hemophilic interactions between adjacent cells to facilitate adhesion as well as mediate extracellular signaling through protein complexes. Studies have identified low E-cadherin levels in poorly differentiated HNSCCs and its low expression to be associated with increased lymphogenous metastasis in HNSCC (Wu et al. 2000; Huber et al. 2011). In addition, meta-analysis of E-cadherin studies in HNSCC showed that abnormal E-cadherin expression is predictive of diminished disease survival (Zhao et al. 2012). N-cadherin is another member of the cadherin family which is upregulated during EMT and has been shown to correlate with malignant behaviors such as high-grade pattern of invasion and poorly differentiated cancer cells in HNSCC (Nguyen et al. 2011). Vimentin is an intermediate filament often used as a mesenchymal marker and is found expressed at sites of cellular elongation and is associated with a migratory phenotype (Zeisberg and Neilson 2009). Vimentin studies directly associated with HNSCC have found its expression to be higher in nodal metastatic cells than in primary HNSCC tumors. Furthermore, downregulation of vimentin by RNA interference decreased proliferation, migration and invasion of metastatic HNSCC cells compared to control (Paccione et al. 2008). In addition, highly metastatic subpopulation of HNSCC cells selected for by 4 rounds of serial metastasis in orthotopic mouse model saw increased vimentin when compared to low expressions in parental control (Yoon et al. 2007). Lastly, fibronectin is a glycoprotein that serves as a scaffold for fibrilar extracellular matrix (ECM) and mediates cellular interactions with the ECM (Zeisberg and Neilson 2009). Fibronectin expression has also been found to correlate with HNSCC and tumor cell aggressiveness. Positive expression was

significantly associated with tumor grade and patients with tumors expressing fibronectin had a trend towards lower overall survival (Mhawech et al. 2005).

1.3 Hepatocyte Growth Factor

1.3.1 Hepatocyte Growth Factor the Cytokine

Hepatocyte growth factor (HGF) also known as scatter factor (SF), is a potent cytokine that can in association with its receptor Met, induce cell proliferation, survival, motility, invasion, and morphogenic changes that stimulate tissue repair and regeneration. While such HGF induced cellular effects are required for normal physiological processes as in normal growth and development and tissue damage repair, inappropriate HGF/Met activation can lead to uncontrolled cell survival, growth, angiogenesis, and metastasis that are essential hallmarks of cancer. HGF/Met activation has been implicated in many types of solid tumors and is often correlated with poor prognosis (Gao and Vande Woude 2005). Because the dysregulation of the HGF/Met signaling pathway has emerged as such a crucial feature of many human malignancies, it provides an important and promising therapeutic target for cancer therapy and a focus for more extensive research.

1.3.2 HGF Involvement in HNSCC

Numerous experimental studies have identified HGF to play a crucial role in the metastatic progression of HNSCC. Biologically, HGF was able to stimulate cell growth, migration, and invasion which was completely blocked with HGF-neutralizing antibody. Furthermore, the use of Met tyrosine kinase inhibitors (TKI) caused 50% reduction of HNSCC tumor growth *in vivo*(Kim et al. 2010). Hasina et al. showed similar results

where invasive capability of HNSCC could be strongly enhanced with HGF which could be abrogated by the use of anti-HGF antibody (Hasina et al. 1999). Moreover, several clinical studies have identified a relationship between the concentration of HGF in serum or in cancer tissue and the progression of disease. HGF concentrations in metastatic HNSCC tissues were significantly higher than those of non-metastatic cancer tissues and normal gingiva as confirmed by measuring protein concentration and performing immunohistochemical staining for HGF in tissue (Uchida et al. 2001; Marshall and Kornberg 1998). Furthermore, serum HGF levels were found to correlate significantly with tumor stage progression with increased levels in advanced stage disease in HNSCC. Interestingly, HGF levels decreased to normal after curative resection of tumors but significantly increased in recurrent HNSCC patients whereas there was no increase in non-recurrent patients (Kim et al. 2007). Such results suggest that HGF plays an important role in the invasion and metastasis of HNSCC and that elevated HGF levels in cancer tissue and patient serum can be used as a predictive marker for tumor grade and metastasis in HNSCC patients. These studies contribute to the now extensive evidence showing that this pathway could be a driving force for the invasive and metastatic potential of HNSCC.

1.3.3 Molecular Biology of the HGF/Met signaling pathway in cancer invasion

HGF, through its receptor Met, is involved in numerous processes and events in the progression of cancer. However, the cytokine complex has the most profound biological effects on the spread of cancer by stimulating its invasive and metastatic capability.

Mechanistically, HGF binding induces MET receptor homodimerization and autophosphorylation of two tyrosine residues, Y1234 and Y1235, within the intracellular domain that activates its catalytic kinase activity (Longati et al. 1994). Additional phosphorylation on the Y1349 and Y1356 tyrosine residues near the COOH terminus forms a multifunctional docking site that recruits a variety of intracellular adaptor proteins such as growth factor receptor bound protein 2 (Grb2), SHC, and Gab1 to mediate further downstream signaling by other downstream effectors (Weidner et al. 1996; Bardelli et al. 1997; Pelicci et al. 1995).

Invading cells require physical degradation of its ECM for efficient movement and optimization of invasion. HGF has been found to have an important role in the upregulation of ECM proteolytic enzymes collectively called matrix metalloproteinases (MMPs) (Fig. 1-4) (Rosenthal et al. 1998; Nabeshima et al. 2000; Monvoisin et al. 2002). Studies show that HGF increases MMP-1, MMP-3, and MMP-9 by inducing the expression of an Ets-oncogene family transcription factor called E1AF in HNSCC resulting in greater invasive ability. Furthermore when cells were transfected with E1AF antisense expression vector, mRNA and protein levels of MMP-1, MMP-3, and MMP-9 decreased and showed lower invasive capability (Hida et al. 1997; Hanzawa et al. 2000). Transcription factor Ets1 transcription and expression levels were also upregulated in response to HGF leading to the expression of MMP-1. Moreover pretreatment of cells with MAPK/ERK inhibitor, blocked HGF mediated up-regulation of MMP-1 suggesting that HGF regulates MMP-1 expression through ERK signaling. Later studies identified Ets1 to be a downstream target of HGF, acting through the MAPK/ERK pathway (Jinnin 2005; Paumelle et al. 2002). But whether the MAPK/ERK signaling

pathway can affect expression of other MMPs as well as what additional upstream signaling pathways can regulate MMP expression in response to HGF, in general, is still not clearly understood.

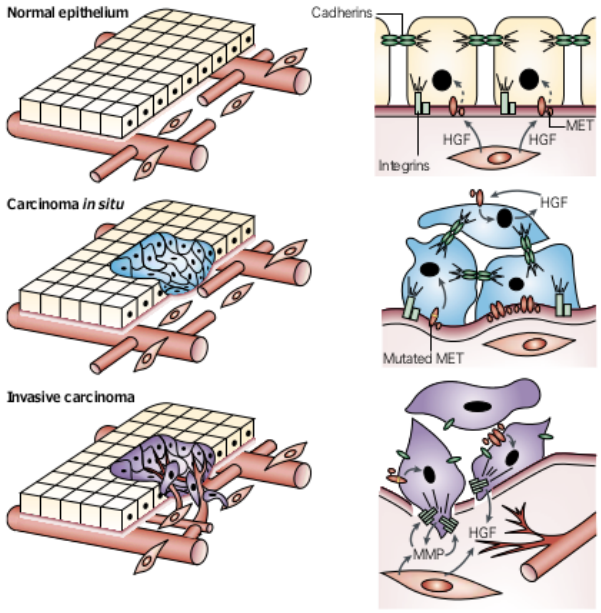

Figure 1-4. Integrins, cadherins, and matrix metalloproteinases as effectors of HGF-dependent invasive growth and angiogenesis. In normal epithelium, MET activation relies on regulated paracrine stimulation from fibroblast-secreted hepatocyte growth factor (HGF). Epithelial cells start proliferating in a non-controlled fashion because of *MET* mutations or the overexpression of HGF. During carcinoma progression, HGF/MET activation leads to tumor disaggregation by disruption of cadherin-based cell–cell junctions. Neoplastic invasion and systemic dissemination occurs due to greater matrix-degrading activity of matrix metalloproteinases (MMPs). (Trusolino and Comoglio 2002)

1.4 Yes Associate Protein

1.4.1 The Hippo Pathway

The Hippo pathway was initially identified in *Drosophilla* to negatively regulate tissue growth. Genetic screens identified Warts (Wts) as the first component of the Hippo pathway. Subsequent studies isolated three additional genes – Hippo (Hpo), Salvador (Sav), and mob as tumor suppressor (mats). Together, these four proteins form the core of the Hippo pathway whereby Hippo interacts with Sav to phosphorylate and activate the complex formed by Wts and Mats. Shortly after in 2005, Yorkie (Yki), a transcriptional coactivator, was identified as the downstream effector of the Hippo pathway which upon phosphorylation by Wts leads to cytoplasmic retention and inactivation. Taken together, these studies showed that activation of the Hippo pathway negatively regulates Yki (Harvey et al. 2013; Bin Zhao et al. 2009).

Components of the Hippo pathway are highly conserved in mammals; Mst1/2 (Hippo homologue), WW45 (Sav homologue), Lats1/2 (Wts homologue), Mob1 (Mats homologue), and YAP (Yki homologue). Accordingly, the mammalian Hippo pathway works similarly as a kinase cascade to negatively regulate YAP. Mst plays an important role by phosphorylating the other three members of the Hippo pathway. Mst1/2 interacts with WW45 through their respective SARAH domains and induces phosphorylation. Mst1/2 was also shown to phosphorylate Mob1and phosphorylate and activate Lats1/2. In turn, activated Lats1/2 can interact directly with and phosphorylate YAP leading to its inactivation by cytoplasmic sequestration thereby effectively suppressing YAP phenotypes, indicating that Lats1/2 is a physiological regulator of YAP and that YAP is its primary target (Fig. 1-5) (Zhao et al. 2010; Bin Zhao et al. 2009).

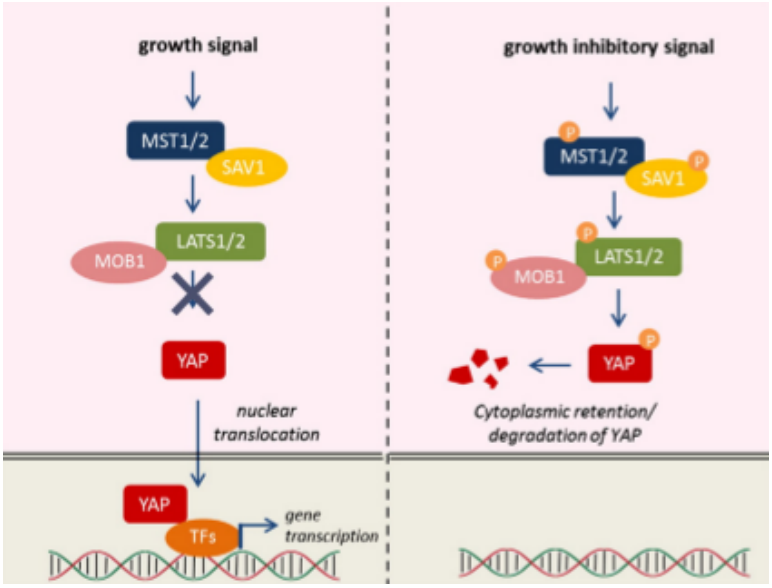

Figure 1-5. Hippo pathway signal transduction in response to growth signals. Left panel: During development, MST1/2 and LATS1/2 remain inactive, allowing YAP translocation into the nucleus to activate genes regulating cell survival and proliferation. Right panel: In response to growth inhibitory signal, active MST1/2 phosphorylates LATS1/2 that sequentially phosphorylates YAP at Ser-127. The phosphorylated YAP is inactivated by cytoplasmic retention and subjected to degradation in the cytoplasm. (Liu et al. 2012)

1.4.2 YAP as a Transcriptional Coactivator

YAP is a transcriptional co-activator which itself has no DNA binding domain, however has several distinct domains with which it interacts with other proteins. It is a 65KDa protein having a proline-rich (P-rich) region at the N-terminal, two WW domains, a Src homology domain 3 binding motif (SH3 BM), a coiled-coil domain (CC), and a C-terminal capped by TWL sequence. In addition, the N-terminus (aa 47-154) of YAP was mapped to be the TEAD binding domain (TBD), and the C-terminus (aa 292-488) was shown to be the activation domain (Zhao et al. 2008a).

The WW domain, a protein-protein interaction module that binds ligands containing the PPXY motif, has been found to be of key importance. PPXY motif is found a wide variety of transcription factors of which ErbB4, Runx2, and p73 have already been identified to bind to YAP through its WW domain. However the most potent YAP target has been identified to be the TEAD family transcription factors to which YAP binds through its TEAD binding domain. Recent studies have shown the importance of TEAD in mediating the biological functions of YAP. TEAD/YAP can induce cell growth, oncogenic transformation, EMT, and invasion in culture (Zhao et al. 2009; 2008b).

1.4.3 YAP as an Oncoprotein

Many recent studies have documented YAP to be a bona fide oncogene. YAP was shown to be in the human chromosome 11q22 amplicon found amplified in numerous solid cancers in organs such as the pancreas, lung, ovary, liver, cervix, as well as in HNSCC (Overholtzer et al. 2006; Zender et al. 2006). Besides genomic amplification, YAP expression was also found elevated in various types of human cancers (MD et al. 2008). Furthermore, YAP overexpression in nontransformed MCF10A mammary tumors was found to induce EMT, suppress apoptosis, and induce anchorage independent growth in soft agar (Overholtzer et al. 2006). More interestingly, transgenic mice with liver specific YAP overexpression showed dramatic increase in liver size which eventually led to tumor formation (Camargo et al. 2007; Dong et al. 2007). These studies combined, strongly indicate YAP to be an oncoprotein.

The oncogenic function of YAP is further supported by inactivation of upstream tumor suppressor components of the Hippo pathway. Lats1 deficient mice developed soft-tissue sarcomas and ovarian stromal cell tumors (John et al. 1999). Mst1/2 deficiency in the liver resulted in massive overgrowth and hepatocellular carcinoma (HCC) (Zhou et al. 2009). Mice heterozygous for WW45 developed tumors including osteosarcoma and HCC (Lee et al. 2008). Moreover loss of expression of Lats1/2 and loss of function mutations of WW45 and Mob have been reported in several cancer cell lines (Tapon et al. 2002; Lai et al. 2005; Jiang et al. 2006).

More specifically, several studies have implicated the importance of YAP in HNSCC. Analysis of human HNSCC tissues suggested YAP expression was elevated in tumors compared to benign tissue, specifically localized at the tumor invasive front. YAP expression in the primary HNSCC tumor was also associated with nodal metastasis. Furthermore, patients with YAP-overexpressing tumors had an overall worse rate of survival than those with non-expressing tumors, and YAP positivity was independently associated with a worse outcome in multivariate analysis (Ge et al. 2011). These results indicated that YAP is a putative oncogene in HNSCC and represents a potential diagnostic and therapeutic target.

CHAPTER 2

METHODS & MATERIALS

2.1 Cell Culture and Reagents

hTERT immortalized but nontransformed human oral keratinocyte cell line OKF6 and human papillomavirus immortalized but nontransformed human oral keratinocyte cell line HOK16B were a kind gift from Drs. Mo Kang and No-Hee Park and cultured in keratinocyte basal medium (KBM) supplemented with KGM bullet kit (Lonza). Human head and neck SCC cell lines SCC1, SCC15, SCC23, and FaDu were cultured in Dulbecco's modified Eagle's medium containing 10% fetal bovine serum and penicillin-streptomycin antibiotics. Recombinant human HGF was purchased from R&D Systems and reconstituted in 0.1% bovine serum albumin in PBS at a concentration of 100μg/μL. All experiments testing HGF were performed at 20ng/mL final concentration, and cells serum starved for 24 hours prior to treatment.

2.2 Viral Transduction

PQCXIH-Myc-YAP and PQCXIH-Myc-YAP-5SA were kindling provided by Dr. K. L. Guan. To create YAP expressing OKF6 (OKF6/YAP) and YAP-5SA expressing OKF6 (OKF6/YAP-5SA) stable cell lines by viral transduction, retrovirus was generated by transfection of PQCXIH-Control, PQCXIH-Myc-YAP or PQCXIH-Myc-YAP5SA into Phoenix 293T packaging cells. 5x10^6 phoenix 293T cells were plated onto 10cm plates 24 hours prior to transfection. For each transfection sample, 20μg of DNA plasmid and 60μL of Lipofectamine 2000 (Invitrogen) were each diluted into 2 separate tubes

containing 1.5mL of Opti-MEM (Invitrogen). After 5 minutes incubation at room temperature, the two tubes were combined, to make a total volume of 3mL, and allowed to incubate at room temperature for 20 additional minutes. 3mL of medium was aspirated from phoenix 293T cells, and the 3mL complex containing DNA plasmid and Lipofectamine 2000, was added drop-wise into the plate containing phoenix 293T cells. After 48 hours post transfection retrovirus was harvested and passed through 0.4μM filter before use. OKF6 cells grown on 6cm plates with 5mL total volume were transduced by triple infection. Every 8 hours, medium was replaced with 4mL fresh KGM with 1mL retrovirus. 48 hours after final transduction, cells were selected for with hygromycin for one week. The surviving cells were pooled and cells expressing protein of interest were confirmed by Western blot analysis.

All shRNAs to create stable knockdown cell lines were cloned into pLKO.1 vector and kindly provided by Dr. K. L. Guan (Table 2-1). For viral transduction, lentivirus was generated by transfection of human embryonic kidney (HEK) 293T. 5x10^6 HEK293T cells were plated onto 10cm plates 24 hours prior to transfection. For each transfection sample, one tube containing 3μg pLKO.1-shRNA or 3μg plKO.1-scramble control along with 2.7μg packaging plasmid pCMV-dR8.2 and 0.3μg envelope plasmid pCMV-VSVG for a total of 6μg DNA in 800μL Opti-MEM, was combined with another tube containing 20μL of Lipofectamine 2000 in 800μL Opti-MEM were combined after 5 minutes incubation at room temperature. After the 1.5mL mixture was incubated for an additional 20 minutes, 1.5mL of medium was aspirated from HEK293T cells, and the 1.5mL complex containing DNA plasmids and Lipofectamine 2000, was added drop-wise into the plate containing HEK293T cells. After 24 hours post

transfection, media was changed with high serum medium containing 30% FBS and incubated for an additional 24 hours at which time lentivirus was harvested and passed through 0.4μM filter before use. SCC cell lines were transduced by adding 1mL virus and polybrene (final concentration at 8μg/ml) directly into culture. 48 hours after transduction, cells were selected for using puromycin selection for one week. The surviving cells were pooled and cells expressing protein of interest were confirmed by Western blot analysis.

2.3 Western Blotting Analysis

All steps for protein extraction were performed at 4^{o}C . Cells were rinsed with ice cold PBS and directly lysed Cells were using RIPA (Radio-immunoprecipitation Assay) buffer (150mM NaCl, 1.0% IGEPAL®, 0.5% sodium deoxycholate, 0.1% SDS, and 50mM Tris, pH 8.0) containing phenylmethylsulfonyl fluoride (PMSF) and protease inhibitor cocktail. Afer 10 minutes incubation, cells were scraped, spun down, and clean protein lysate separated from debris.

Cell lysates were run on 12.5% SDS polyacrylamide gel and transferred to polyvinylidene difluoride membrane (PVDF) using semidry transfer apparatus (Bio-Rad). Membranes were blocked with 5% milk in TBST for one hour and incubated with primary antibodies overnight in 4^{o}C. Membranes were washed with TBST for 10 minutes 3 times, followed by incubation with horseradish peroxidase (HRP)-conjugated anti-rabbit or anti-mouse immunoglobulin G (IgG) (Promega) in 5% milk in TBST for 1 hour at room temperature. After membranes were washed with TBST for 10 minutes 3

times, immunocomplexes were envisioned with SuperSignal reagents (Pierce). Please refer to Table 2-2 for list of antibodies.

2.4 RNA extraction and cDNA synthesis

Total RNA was isolated using TRIzol reagent (Invitrogen) following manufacture's procotol. Briefly, medium was removed and 1mL TRIzol reagent added per $10cm^2$, and allowed to incubate at room temperature for 5 minutes to allow complete dissociation of nucleoprotein complexes. 200μL of chloroform was added per 1mL TRIzol reagent used and vortexed for 15 seconds. Samples were incubated at room temperature for 3 minutes before centrifugation at 12,000g for 15 minutes at 4^oC for phase separation. The upper aqueous phase was collected and 500μL isopropyl alcohol was added per 1mL TRIzol reagent volume used to each sample to precipitate RNA. Samples were incubated at room temperature for 10 minutes, and centrifuged at 12,000g for 10 minutes at 4^oC. After aspirating the supernatant, 1mL of 75% EtOH was added, gently vortexed and centrifuged at 10,000g for 5 minutes at 4^oC. Samples were aspirated and allowed to air dry before dissolving the RNA pellet in 100μL of ultrapure water.

Complementary DNA (cDNA) was synthesized with oligo(dT) primers using Moloney murine leukemia virus reverse transcriptase (M-MuLV RT) (New England Biolabs) following manufacture's protocol. Briefly, 1ug of RNA was combined with oligo(dT), and dNTP mix in a 16μL total reaction volume, which was heated for 5 minutes. The RNA/primer/dNTP mix was then combined with Murine RNase inhibitor, M-MuLV reverse transcriptase, and RT buffer to make a final reaction volume of 20uL.

Each sample incubated at 42^{o}C for 1 hour, followed by 80^{o}C for 5 minutes, and then brought 800uL final volume with ultrapure water.

2.5 Real-Time PCR

Quantitative RT-PCR analysis was carried out with iQ SYBR Green Supermix (BioRad) on an iCycler iQ real-time PCR detection system (BioRad). *GAPDH* levels were used as a loading control for rea-time PCR. Sequences of primer pairs used are listed in **Table 2-3**.

2.6 Microarray and WGCNA

For microarray, total RNA was extracted with miRNeasy kit following the manufactureer's protocol (Qiagen). 5ug aliquots of total RNA were submitted to the University of California, Los Angeles, (UCLA) DNA Microarray Facility, for further processing and hybridization to Affymetrix Human 1.0 ST Array. The array was scanned with GeneArray scanner (Affymetrix) and robust multichip average (RMA) method was used to normalize the raw data.

Analysis of microarray data at a network level was performed using the weighted gene correlation network analysis (WGCNA) along with its functions in the WGCNA library done in the free statistical package R (Langfelder and Horvath 2008). Clusters of genes that behave similarly between sample conditions, termed module eigengenes, were grouped together into different color modules.

2.7 Proliferation assay

Cells were seeded into a 24 well plate. 500µl fresh culture medium was replaced every 2 days. Cell proliferation was measured by one of two methods. Cells were detached with trypsin and counted daily using trypan blue with hemacytometer. Or, MTT (3-(4,5-dimethylthiazol-2-yl)-2,5-diphenyltetrazolium bromide) assay was performed. 10% volume of 12mM MTT stock solution in sterile PBS, was added directly into culture medium and incubated at 37^{o}C for 3 hours. After removing the medium, DMSO (dimethylsulfoxide) was added and incubated for an addition 10 minutes at 37^{o}C**.** Solution was then mixed and absorbance measured at 570 nm.

2.8 Foci formation assay

For foci formation assay, 5x10^{5} cells were seeded onto 50mm dishes and culture medium replaced every 2 days. Cells were washed with ice cold PBS then fixed with ice cold methanol for 10 minutes. Methanol was aspirated and replaced with 0.5% crystal violet solution in 25% methanol and incubated at room temperature for 10 minutes after which plates were rinsed with water and allowed to air dry.

2.9 Invasion Assay

To test cell invasion, cells were plated onto the top chamber of BD BioCoat Matrigel Invasion Chambers in 500µL total volume of serum free DMEM. 750µL of DMEM 0.1% FBS in the bottom chamber used as a chemoattractant. Chambers were incubated in 37^{o}C overnight after which matrigel was removed and invading cells stained

using HEMA 3 kit (Fisher). For invasion assays testing HGF, the addition of HGF was made to bottom chambers.

2.10 Soft Agar Assay

For soft agar colony formation assay, $2x10^4$ cells in culture medium was mixed with an agar solution in PBS to form a 2 ml top layer at 0.3% agar which was layered over a solidified 0.6% agar 2 ml bottom layer in a 6 well plate. 2 ml growth medium was replenished every 3 days until colonies were imaged and counted.

2.11 In Vivo Subcutaneous Injection

All animal experiments were performed in accordance with protocol approved by the UCLA Committee on Animal Care. To perform subcutaneous injections, cell concentration was adjusted to $1x10^6$ cells in 100μL ice cold PBS. 100μL of cells containing 1x10^6 cells was subcutaneously injected using 27 gauge needle into the left and right flanks of mice. Tumor growth was measured according to experimental design after which mice were sacrificed and tumors isolated.

2.12 Immunohistochemistry

Tumor specimens were paraffin-embedded and sectioned at UCLA Translational Pathological Core Laboratory. Tissue sections were deparaffinized with two washes in xylene for 5 minutes each and rehydrated with distilled water through an ethanol series for 10 minutes each. Tissue antigens were retrieved in citrate buffer (2.1g/L citric acid, pH 6.0) with incubation at 120^oC for 20 minutes by pressure cooking. Tissue sections

were pre-incubated with 3% hydrogen peroxide block solution for 10 minutes and incubated with antibodies against YAP and Myc, or control IgG at 4^{o}C overnight. Tissue sections were then incubated with HRP-labeled polymer for 60 min, detected the immunocomplexes with AEC+ chromogen (Dako EnVision System), and counterstained with hematoxylin QS.

shRNA	Sequence
YAP shRNA #1 - sence	5’ - CCGGCTGGTCAGAGATACTTCTTAACTCGAGTTAAGAAGTATCTCTGACCAGTTTTTC – 3’
YAP shRNA #1 - antisence	5 - AATTGAAAAACTGGTCAGAGATACTTCTTAACTCGAGTTAAGAAGTATCTCTGACCAG - 3’
YAP shRNA #2 - sence	5 - CCGGAAGCTTTGAGTTCTGACATCCCTCGAGGGATGTCAGACTCAAAGCTTTTTTTC – 3’
YAP shRNA #2 - antisence	5 - AATTGAAAAAAAGCTTTGAGTTCTGACATCCCTCGAGGGATGTCAGAACTCAAAGCTT – 3’
TEAD1/3/4 shRNA #1 - sence	5 - CCGGATGATCAACTTCATCCACAAGCTCGAGCTTGTGGATGAAGTTGATCATTTTTTC – 3’
TEAD1/3/4 shRNA #1 - antisence	5 - AATTGAAAAAATGATCAACTTCATCCACAAGCTCGAGCTTGTGGATGAAGTTGATCAT – 3’
TEAD1/3/4 shRNA #2 - sence	5 - CCGGGATCAACTTCATCCACAAGCTCTCGAGAGCTTGTGGATGAAGTTGATCTTTTTC – 3’
TEAD1/3/4 shRNA #2 - antisence	5 - AATTGAAAAAGATCAACTTCATCCACAAGCTCTCGAGAGCTTGTGGATGAAGTTGATC – 3’

Table 2-1. shRNAs used for lentivirus to create stable cell lines

Table 2-2. Antibodies used for Western blot analysis and immunohistochemistry

Antibody	Manufacturer	Stock	Dilution
YAP	Santa Cruz Biotechnology	200µg/ml	1:1000
E-cadherin	Cell Signaling Technology	NA*	1:1000
N-cadherin	Cell Signaling Technology	NA*	1:1000
Vimentin	Cell Signaling Technology	NA*	1:1000
c-Myc	Santa Cruz Biotechnology	200µg/ml	1:1000
α-tubulin	Sigma-Aldrich	2.5-6mg/ml	1:100,000

* Cell Signaling Technology stock antibody concentrations not provided by manufacturer

Table 2-3. Primer sequences used in RT-PCR

Gene	Orientation	Primer sequence 5'→3'
GAPDH	Forward	ATCATCCCTGCCTCTACTGG
	Reverse	GTCAGGTCCACCACTGACAC
MMP3	Forward	TGGCATTCAGTCCCTCTATGG
	Reverse	AGGACAAAGCAGGATCACAGTT
IL6	Forward	TCTCCACAAGCGCCTTCG
	Reverse	CTCAGGGCTGAGATGCCG
IL1A	Forward	ATCCTGAATGACGCCCTC AA
	Reverse	TGGATGGGCAACTGATGTGA
SMURF2	Forward	TGGATCAGGAAGTCGGAAAA
	Reverse	GGACATGTCTAACCCCGGA
KRT5	Forward	CTGGTCCAACTCCTTCTCCA
	Reverse	GGAGCTCATGAACACCAAGC
FAT2	Forward	GCTGCTGGGCTGTAGATAGG
	Reverse	AGCTCCAAAGGGAAGCTGAC
TEAD1	Forward	CTTGAATGTGCAATGAAGCG
	Reverse	CGAAGTTTGCCTCGGACTC
TEAD2	Forward	CTCACTCCGTAGAAGCCACC
	Reverse	TGCCTTCTTCCTGGTCAAGT
TEAD3	Forward	GCACCTTCTTCCGAGCTAGA
	Reverse	TACGGCCGAAATGAGTTGAT
TEAD4	Forward	GCTCCACTCGTTGGAGGTAA
	Reverse	GGACTCCTTGGAACTGGCTT

SPECIFIC AIMS AND HYPOTHESES

YAP is most often considered an oncogene. Numerous studies have identified its transformative potential. However, the few but conflicting studies that suggest YAP to acts as a tumor suppressor can not be overlooked, and indicates that whether YAP takes on the role of oncogene or tumor suppressor may be tissue context dependent. Whether YAP is important in, or what role it plays with respect to HNSCC is still not clear. Moreover, an association between YAP and HGF, a cytokine implicated to play an important role in all stages of cancer progression, particularly the invasive growth program, has yet to be identified. Our overall objective is to determine whether YAP serves as an oncogene in HNSCC, and if so, whether it can mediate HGF induced gene expression. Our results will be expected to have important implications in the understanding and design of therapeutic approaches to prevent HNSCC progression as well as identify a new method by which HGF gene expression is regulated.

SPECIFIC AIM 1: Identify whether YAP plays an oncogenic role in the progression towards cancer of oral keratinocytes

In this aim, we will establish whether overexpression of YAP in immortalized but nontransformed human oral keratinocyte cell line, OKF6, can induce cellular transformation. YAP and a constitutively active YAP, YAP-5SA, overexpressing OKF6 stable cell lines will be generated to investigate transformation capability, by testing for EMT, proliferation, and invasion. We will also confirm our *in vitro* findings *in vivo* by performing subcutaneous injections into nude mice.

SPECIFIC AIM 2: Determine whether YAP is necessary for the proliferative and invasive growth of HNSCC

In this aim, we will identify whether YAP knockdown can inhibit proliferation and invasion of HNSCC. YAP knockdown HNSCC stable cell lines will be created and biological experiments testing proliferation and invasion performed. Furthermore, correlation between YAP and HNSCC stage will be evaluated by testing for YAP abundance in HNSCC tissue samples of varying stage.

SPECIFIC AIM 3: Determine whether YAP regulates HGF mediated cellular response in HNSCC

In this aim, we will identify whether YAP is necessary for HGF mediated cellular response. Furthermore we will attempt to identify specific genes that may be important in and exclusive to YAP activity upon HGF stimulation. Using YAP knockdown HNSCC stable cell lines, we will perform biological tests as well as perform microarray following HGF stimulation.

CHAPTER 3

YAP INDUCES TRANSFORMATIVE PROPERTIES OF HUMAN ORAL KERATINOCYTES

RESULTS

3.1 YAP Expression Induces EMT of OKF6

YAP is an oncogene found amplified in HNSCC as well as numerous other solid cancers including lung, breast, and colon (Overholtzer et al. 2006; Zender et al. 2006). Its expression is associated with organ size control, proliferation, growth, metastasis, and stem cell renewal (Harvey et al. 2013; Zhao et al. 2010). More specifically, YAP protein expression has been found increased in HNSCC, primarily at the tumor invasive front, and its expression in primary HNSCC has been associated with nodal metastasis (Ge et al. 2011). To determine the affects of YAP expression in oral keratinocytes, we created stable cell lines in hTERT immortalized but nontransformed human oral keratinocyte cell line OKF6. YAP and constitutively active mutant YAP, YAP-5SA, expression in OKF6 were confirmed by Western blotting analysis (Fig. 3-1A). Inspection under light microscope revealed a dramatic change in morphology. Whereas control cells displayed cuboidal epithelial like cellular morphology, YAP and YAP-5SA expressing cells displayed a more dedifferentiated, spindle like, mesenchymal morphology (Fig. 3-1B). This change in morphology is indicative of epilthelial to mesenchymal transition (EMT), a process that occurs as a benign tumor progresses to become a malignant tumor. EMT was confirmed by reduction of epithelial marker E-cadherin, and the gain of mesenchymal markers N-cadherin and vimentin by Western blotting analysis, and further

confirmed at mRNA expression level by quantitative PCR (qPCR) (Fig. 3-1, C and D). Taken together, our results show that YAP and YAP-5SA can induce EMT in OKF6 cells.

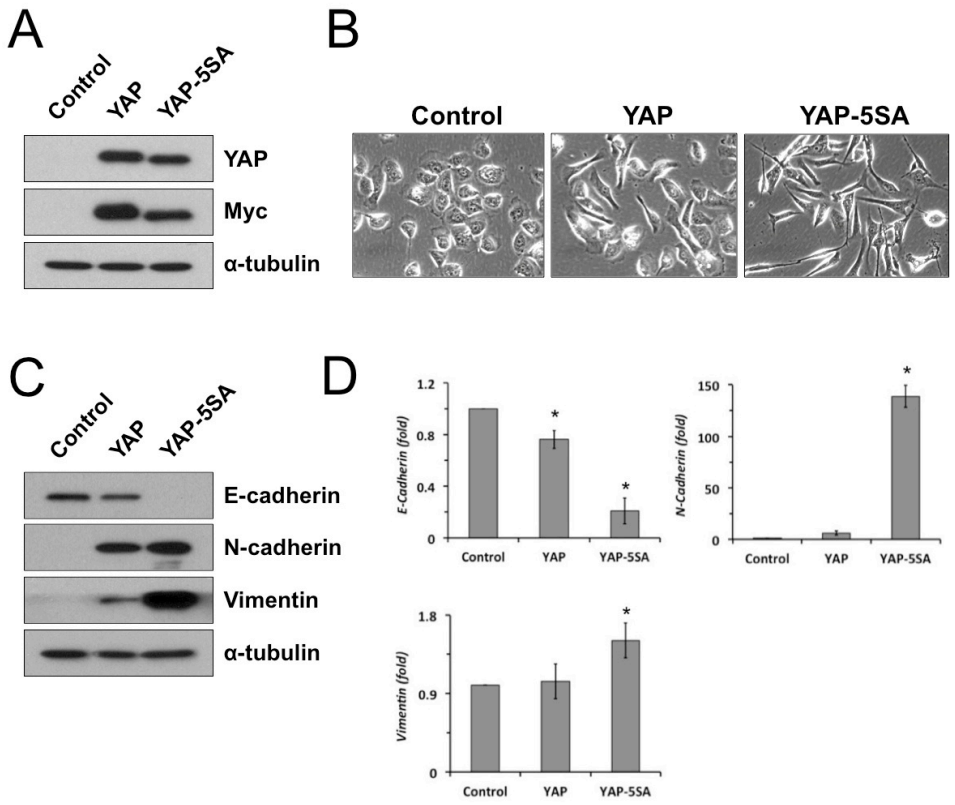

Figure 3-1. YAP-5SA induces EMT. (A) YAP and YAP-5SA expression was confirmed by western blot analysis. OKF6 cells were retrovirally infected using virus containing control, YAP-Myc, or YAP-5SA-Myc expressing pQCXIH plasmids and selected for using hygromycin. (B) YAP expression induces morphological change on monolayer cultures. Representative brightfield images of cells growing in monolayer cultures are shown at 40x magnification. (C) Expression of YAP-5SA results in loss of epithelial markers and gain of mesenchymal markers. Western blot analysis reveals decrease in epithelial maker E-cadherin and increase mesenchymal markers N-cadherin and vimentin. (D) Western blot results for EMT markers were confirmed by qPCR. Results were normalized to GAPDH. Data are means ± SD of triplicate samples from a representative experiment. *$p < 0.01$, unpaired two-tailed Student's *t* test.

3.2 YAP Expression Induces Proliferative Advantage and Increases Invasive Potential

To further test the transformative effects of YAP expression, we assessed its effects on cell proliferation. YAP and YAP-5SA displayed faster initial proliferation when compared to control (Fig. 3.2A). In addition, YAP expressing cells achieved confluence faster than control. More interestingly, YAP-5SA was able to cause continued proliferation past confluence (Fig. 3-2A), indicating the possibility of these cells to overcome cell contact inhibition. Therefore, to more clearly determine the effects of YAP expression on contact inhibition, we performed foci formation assay. Whereas control and YAP expressing cells were unable to form foci, YAP-5SA was able to form numerous foci (Fig. 3-2B). These results show that YAP-5SA but not YAP can cause OKF6 cells to overcome contact inhibition and proliferate in multilayers.

The ability of cells to grow in suspension, unattached to a surface, is another hallmark characteristic of cellular transformation (REF). To identify whether YAP expression could allow for anchorage-independent growth, we performed soft agar assay. Although very small colonies could be formed after 16 days by YAP expressing cells, significantly more colonies, larger and distinct formed within 10 days for cells expressing YAP-5SA (Fig. 3-3 A and B). We also tested the invasive capability of these cells using matrigel invasion chambers, and our results indicate a dramatic increase in invasion of YAP and YAP-5SA expressing cells compared to control (Fig 3-3C). Our results show that YAP-5SA can cause anchorage-independent growth and increase invasive capability of OKF6 cells.

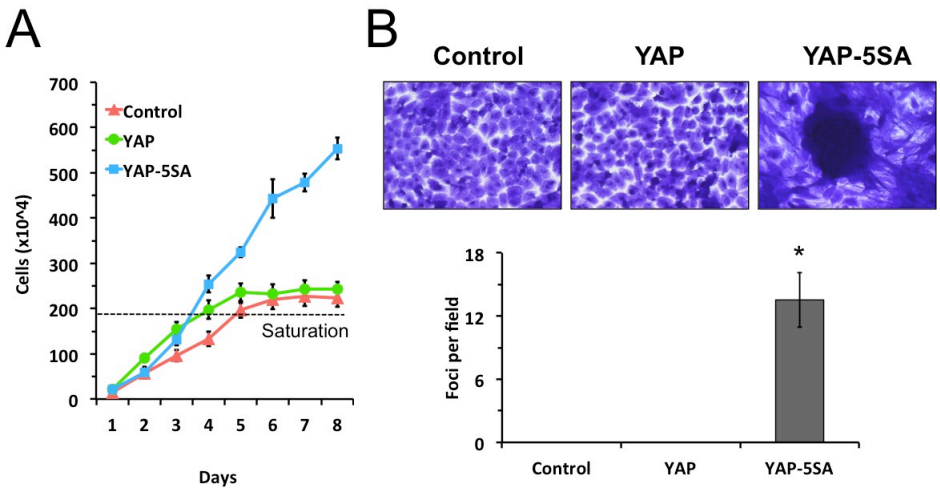

Figure 3-2. YAP-5SA promotes proliferation and allows loss of contact inhibition. (A) YAP and YAP-5SA expression increased proliferative rate and saturation density. Control, YAP, and YAP-5SA OKF6 cells were grown in parallel and cell number was determined daily using trypan blue over an 8-day timecourse. (B) YAP-5SA induced OKF6 cells to overcome contact inhibition. Control, YAP, and YAP-5SA OKF6 cells were grown beyond confluence for 1 week and foci-formation assay performed. (Top) Representative brightfield images. 40x magnification (*Bottom*) Data is the mean number of colonies per field of 5 10X images. (n=3 independent experiments).

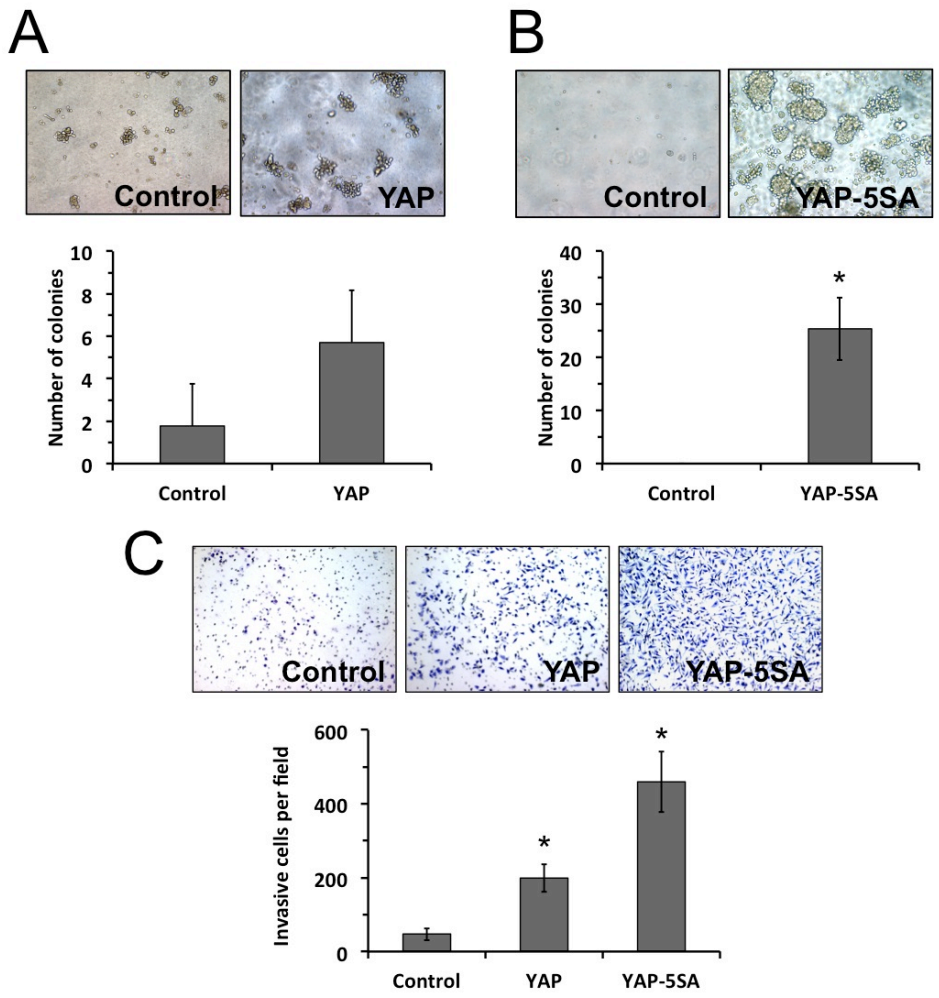

Figure 3-3. YAP-5SA induces anchorage independent growth and invasion. (A) YAP expression induces anchorage independent growth in soft agar. Cells were grown in agar suspension for 16 days. (*n*=3 independent experiments). (*Top*) Representative brightfield images (*Bottom*) Data is the mean number of colonies per 10X field of 5 images. (B) YAP-5SA expression induces anchorage independent growth in soft agar. Cells were grown in agar suspension for 7 days. (*n*=3 independent experiments). (Top) Representative brightfield images. (*Bottom*) Data is the mean number of colonies per 10X field of 5 images. (C) YAP induces invasion. Control, YAP, and YAP-5SA cells were plated onto 8μM transwelll invasion chambers and allowed to invade for 24 hours. (*Top*) Representative brightfield images. (Bottom) Data is the mean number of colonies per 10X field. (*n*=3) Data are means ± SD of triplicate samples from a representative experiment. *$p < 0.01$, unpaired two-tailed Student's *t* test.

3.3 YAP Expression Induces Tumor Development and Growth *In Vivo*

We validated our in vitro findings *in vivo* by performing subcutaneous injections in nude mice. Control or YAP-5SA expressing OKF6 cells were injected into flanks of mice and sacrificed 26 days post injection. Our results indicate that YAP-5SA cells can induce the growth and formation of tumors *in vivo* (Fig. 3-4A). Not only did YAP-5SA tumors continue to grow, but these cells also showed 100% incidence of tumor formation compared to 0% control (Fig 3-4B). Excised tumors were stained with H&E to confirm tumor formation and immunohistochemistry performed to confirm YAP and Myc expression (Fig. 3-4C). Our *in vivo* experiment validated the transformative capability made evident by YAP-5SA expression *in vitro.*

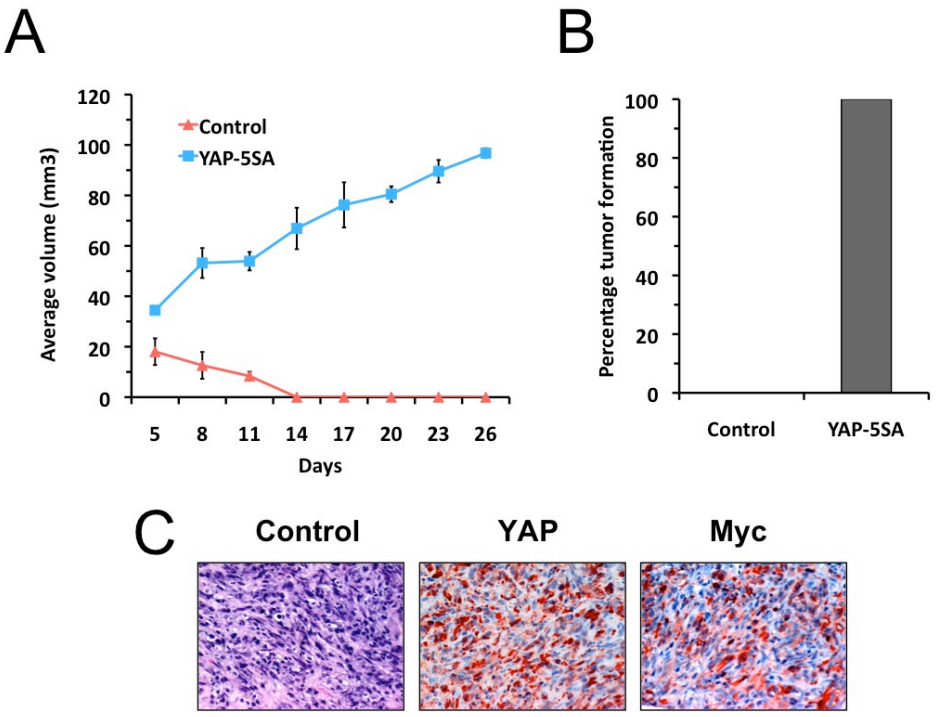

Figure 3-4. YAP-5SA promotes tumor formation and progression *in vivo*. (A) YAP-5SA induced the formation of tumors in nude mice. 1x10^6 control and YAP-5SA OKF6 cells in 100µL were subcutaneously injected into nude mice. (B) YAP-5SA expression caused 100% tumor formation compared to no tumor formation of control OKF6 cells. (C) Histological analysis of excised tumors indicate formation of tumors. YAP-5SA expression was confirmed by immunohistochemistry.

DISCUSSION

In this study we report that expression of constitutively active YAP, YAP-5SA, in hTERT immortalized but nontransformed human oral keratinocyte cell line, OKF6, results in morphological changes that are hallmarks of tumorigenic transformation. YAP-5SA expression in OKF6 induced EMT and allowed for increase in proliferation, invasion, and resistance to apoptosis. Our findings indicate that active YAP may contribute to the malignant transformation of normal keratinocytes and underlies the important role that YAP may play in tumor formation and malignant progression towards oral cancer.

Expression of YAP and to a greater extent YAP-5SA induced morphological changes indicative of EMT, an important process that leads to greater proliferative, invasive, and metastatic potential (Gupta and Massagué 2006; Talbot et al. 2012). Whereas control cells displayed cuboidal epithelial morphology, YAP and YAP-5SA expression caused cells to become progressively more mesenchymal in morphology, displaying greater elongation and loss of cell-cell contact. Downregulation of E-cadherin is one of the essential leading events for EMT and is considered a hallmark of this process, and at present is one of the most reliable markers of EMT. YAP expression clearly reduced E-cadherin protein expression whereas YAP-5SA resulted in complete loss of E-cadherin. qPCR confirmation was consistent with protein expression levels, suggesting that YAP can regulate E-cadherin at a transcriptional level. Mesenchymal markers N-cadherin and vimentin increased as expected, with greater expression in OKF6/YAP-5SA which is also consistent with the constitutively active state of YAP, as opposed to the lack of expression in control. YAP expression in our OKF6 cell line also

resulted in a proliferative advantage over the course of 5 days. More interestingly, whereas control and OKF6/YAP ceased to proliferate upon reaching saturation, OKF6/YAP-5SA continued to proliferate, indicating that active YAP can cause normal cells to overcome cell-cell contact inhibition, a process by which cells can restrict cell proliferation and migration. Our *in vitro* proliferation results were positively reflected *in vivo* where 100% tumor formation was obtained using OKF6/YAP-5SA compared to no tumor formation using control. Concomitantly OKF6/YAP and to a greater effect OKF6/YAP-5SA displayed significant increase in invasive capability. Furthermore, overcoming anchorage independent growth, another important process in metastatic progression, was also displayed with the expression of YAP and YAP-5SA.

The inappropriate proliferation and invasion of normal cells in becoming malignant cancers is challenged by multiple layers of mechanisms that suppress tumor formation and metastasis (Leemans et al. 2010; Hanahan and Weinberg 2011). Although numerous studies involving mouse models and human cancer cell lines have identified YAP to be a potent oncogene, whether YAP plays an oncogenic role in oral cancer and the mechanism by which it can transform normal cells is still unclear. Our results indicate that YAP can transform human oral keratinocytes and may do so by down-regulating E-cadherin. E-cadherin is a transmembrane protein that interacts in a homophilic manner with E-cadherin molecules on the surface of neighboring cells to form adherins junctions, particularly of the epithelium (Bogenrieder and Herlyn 2003). E-cadherin adhesive functions not only physically block movement of cells and facilitate other cell-cell interactions, but also functions in cellular signaling (Wheelock and Johnson 2003). YAP has previously been found to induce the expression of several E-cadherin

transcriptional repressors such as snail, twist, and sox (Liu et al. 2010b; Lamar et al. 2012). Furthermore, the TEAD transcription family have recently been identified to play a critical role in mediating YAP-dependent gene induction, and therefore it is possible that activated YAP in conjunction with TEAD can cause expression of negative regulators to suppress E-cadherin expression leading to the transformation of normal cells.

The functional regulation of E-cadherin by YAP has important implications in the transformation of normal cells in cancer biology. E-cadherin is a key tumor suppressor that mediates extracellular signaling to regulate cell growth, survival, and invasion (Huber et al. 2011; Zhao et al. 2012; Huang 2008). A link between YAP and E-cadherin would reveal how YAP could induce cell transformation by regulating extracellular signaling cues. Given the prominent role of YAP and E-cadherin in tumorigenesis, it will be interesting to explore the interaction these genes may play in human cancer.

CHAPTER 4

YAP KNOCKDOWN INHIBITS CANCER CHARACTERISTICS IN HNSCC

RESULTS

4.1 YAP Knockdown Inhibits Proliferation and Invasion of HNSCC

Previously, we have shown that YAP can induce proliferation and invasion of human oral keratinocytes. To determine whether knockdown of YAP can inhibit cell proliferation and invasion in SCC, we created stable cell lines with knocked down of YAP using two lentiviral-based short hairpin RNAs (shRNAs; sh1 and sh2) targeting two different YAP sequences in SCC23. Both YAPsh1 and YAPsh2 were able to knockdown YAP protein expression in SCC23 (Fig. 4-1A). Furthermore, when grown in 2D plastic culture, SCC23 with YAP knockdown by both YAPsh1 and YAPsh2 developed more epithelial-like morphology, growing as tightly coherent islands of cells with smooth external borders that lacked any cellular projections (Fig. 4-1B). This is in contrast to the elongated or angular morphology of control cells which had spike like projections. Proliferation assay performed over 5 days indicated that YAP can inhibit cell proliferation (Fig. 4-1C). There was no difference in cell proliferation between control, SCC23/YAPsh1, and SCC23/YAPsh2 cells over 48 hours, but SCC23/YAPsh1 and SCC23/YAPsh2 cells grew more slowly then control cells after 72 hours. By the end of the experiment at day 5, there was significantly more cells in control compared to total cell number in either SCC23/YAPsh1 or SCC23/YAPsh2. YAP knockdown also greatly inhibited invasive capability of SCC23 (Fig. 4-1D). Moreover, using SCC23/YAPsh1, we found that knockdown of YAP can greatly inhibit SCC tumor growth *in vivo* when

subcutaneously injected into nude mice. Not only did YAP knockdown inhibit formation of tumors, but it also caused a reduction in the size of tumors formed (Fig. 4-1E).

To determine whether our findings for YAP applied to additional SCC cell lines, we checked basal YAP expression levels of SCC1, SCC15, and FaDu compared to an hTERT immortalized but nontransformed oral keratinocyte cell line HOK16B (Fig. 4-2A). Based on our results, we knocked down YAP in SCC1. Knockdown of YAP in SCC1 was confirmed by Western blot analysis (Fig. 4.2B). Unlike SCC23, there was no discernable difference in morphology between control, SCC1/YAPsh1, and SCC1/YAPsh2 (Fig. 4-2C). Consistent with YAP knockdown in SCC23, SCC1/YAPsh1, and SCC1/YAPsh2 showed decrease in cell proliferation rate compared to control (Fig. 4-2D). By the end of the experiment at day 5, there was significantly more cells in control compared to total cell number in either SCC1/YAPsh1 or SCC1/YAPsh2. YAP knockdown also inhibited invasive capability of SCC1 (Fig. 4-2E). Taken together, our results indicate that YAP plays an important role in promoting growth and invasion of HNSCC.

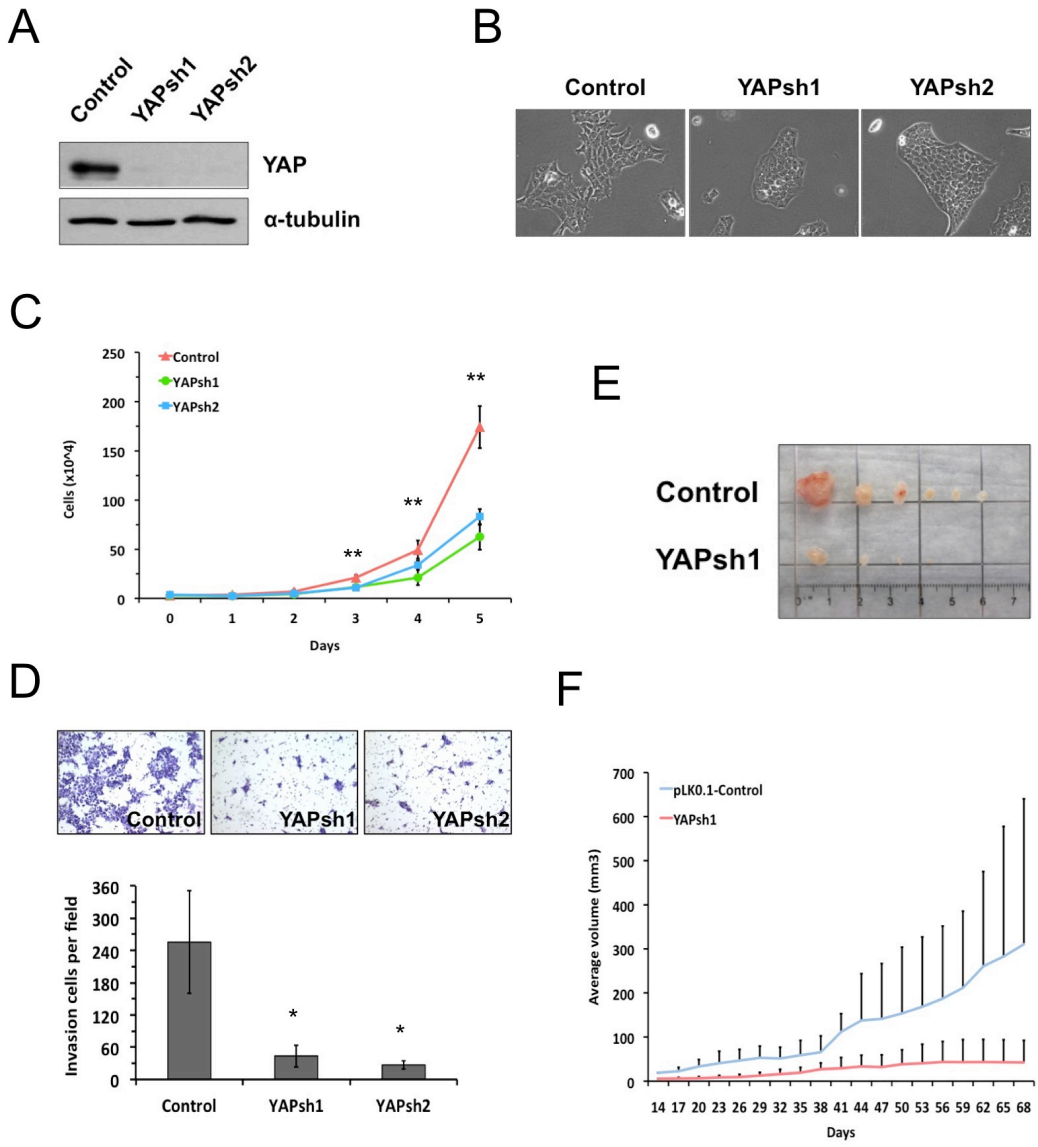

Figure 4-1. Knockdown of YAP inhibits SCC23 growth and invasion. (A) Western blot analysis for YAP expression in SCC23 stably expressing one of two shRNA vectors targeting YAP (YAPsh1, YAPsh2) or nontargeted (Control) vector. (B) Representative brightfield microscopy images described in (A). (C) Cell proliferation analysis of cells described in (A). $^{**}P < 0.05$, unpaired two-tailed Student's *t* test (n=3). (D) Analysis of invasion using cells described in (A). (Top) Representative brightfield images. (Bottom) Data are means ± SD of triplicate samples from representative experiments (n=3). $^{*}P < 0.01$, unpaired two-tailed student's *t* test. (E and F) Tumors resulting from subcutaneous injections of SCC23/Control and SCC23/YAPsh1. Data are means ± SD (two separate injection of each mouse with 5 mice in each group) of representative of one experiment (*n*=1 experiment).

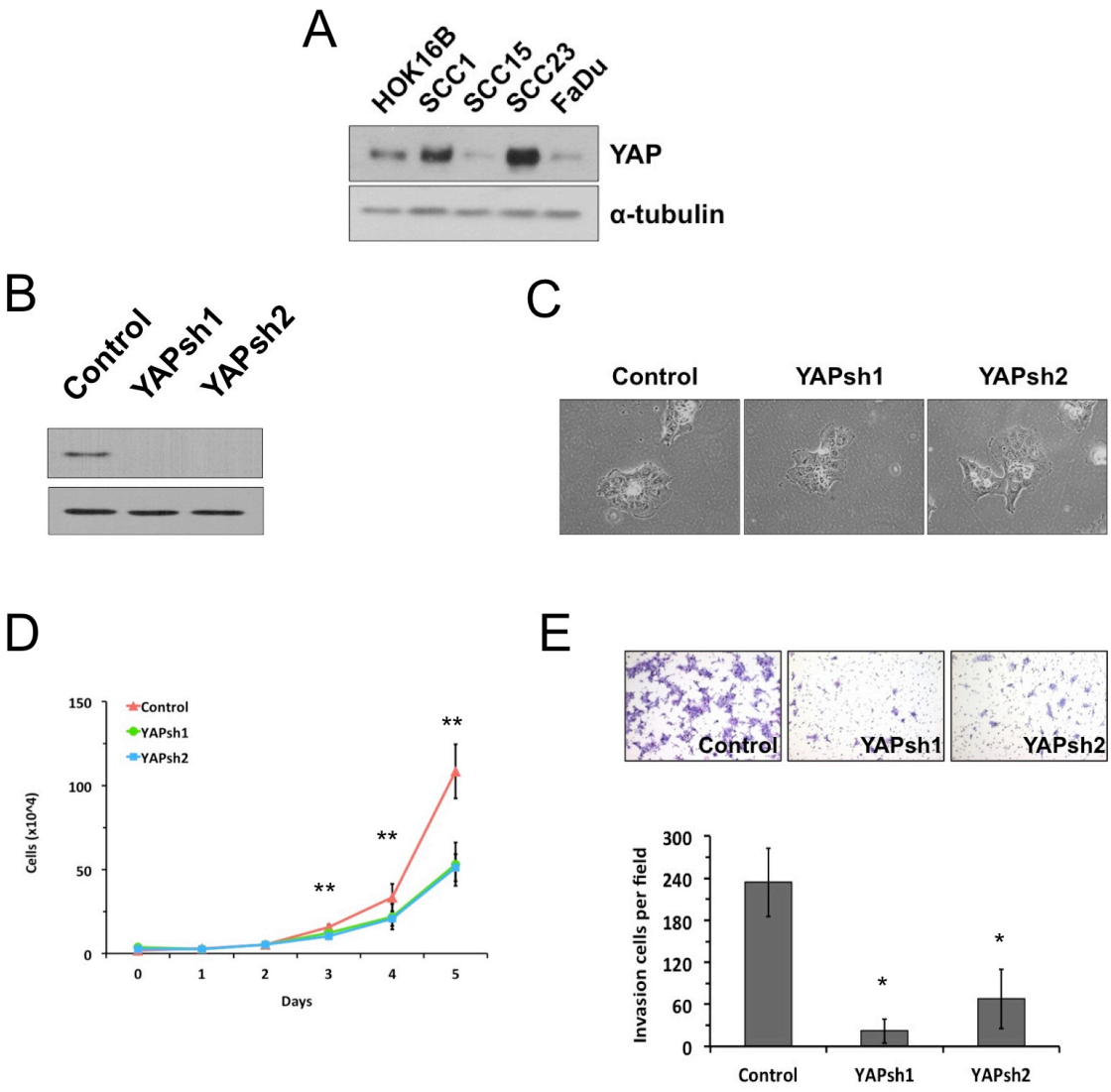

Figure 4-2. Knockdown of YAP inhibits SCC1 growth and invasion. (A) Western blot analysis for YAP expression in SCC23 stably expressing one of two shRNA vectors targeting YAP (YAPsh1, YAPsh2) or nontargeted (Control) vector. (B) Representative brightfield microscopy images described in (A). (C) Cell proliferation analysis of cells described in (A). $^{**}P < 0.05$, unpaired two-tailed Student's *t* test (n=3). (D) Analysis of invasion using cells described in (A). (Top) Representative brightfield images. (Bottom) Data are means ± SD of triplicate samples from representative experiments (n=3). $^{*}P < 0.01$, unpaired two-tailed student's *t* test. (E and F) Tumors resulting from subcutaneous injections of SCC23/Control and SCC23/YAPsh1. Data are means ± SD (two separate injection of each mouse with 5 mice in each group) of representative of one experiment (*n*=1 experiment).

4.2 YAP Abundance Correlates With Lymph Node Metastasis in Human HNSCC

To further determine whether YAP can promote human SCC progression and metastasis, we compared the abundance of YAP by immunohistochemistry in four tissue types: adjacent normal epithelial tissue (Normal), primary SCC tissue with no lymph node metastases (SCC –LN), primary SCC tissue with lymph node metastases (SCC +LN), and lymph nodes with SCC metastases (LN). YAP abundance was significantly higher in SCC -LN compared to Normal (Fig. 4-3 and Table 4-1). Furthermore, YAP abundance was significantly increased in SCC +LN and LN when compared to SCC –LN. However there was no difference in the high abundance of YAP between SCC +LN and LN, indicating that YAP expression is sustained once SCC are capable of metastasis and remain elevated after having colonized regional lymph nodes. Our results suggest that YAP expression and abundance is correlated with cancer status and stage in HNSCC and that YAP may play an important role in cancer formation, progression, and metastasis of HNSCC.

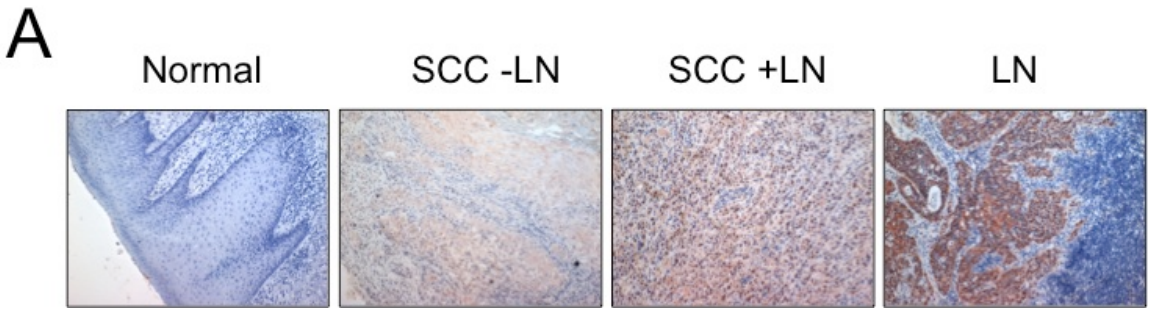

Figure 4-3. Immunohistochemistry for YAP abundance in human HNSCC tissue. Human SCC with no lymph node metastasis tissue (SCC-LN), SCC with lymph node metastasis tissue (SCC+LN), SCC lymph node metastasis tissue (LN), compared with adjacent normal epithelial tissue (Normal). Images are representative of 44 (Normal), 34 (SCC-LN), 34 (SCC+LN), and 34 (LN) samples.

	Normal	SCC-LN*	SCC+LN**	LN
0	47.73%	20.59%	11.76%	5.88%
	(21/44)	(7/34)	(4/34)	(2/34)
+	43.18%	47.06%	20.59%	23.53%
	(19/44)	(16/34)	(7/34)	(8/34)
++	9.09%	23.53%	44.12%	38.24%
	(4/44)	(8/34)	(15/34)	(13/34)
+++	0.00%	8.82%	23.53%	32.35%
	(0/44)	(3/34)	(8/34)	(11/34)

*$P < 0.01$ SCC-LN versus normal, Wilcoxon rank sum test.

**$P < 0.01$ SCC+LN versus SCC-LN, Wilcoxon rank sum test.

Table 4-1. YAP is highly abundant in human SCC lymph node metastasis. Normal human adjacent epithelial tissues (Normal; n=35), human primary SCC without lymph node metastasis (SCC-LN; n=34), human primary SCC without lymph node metastasis (SCC+LN; n=34), and metastatic SCC in lymph node (LN; n=34) were stained for YAP. The staining intensity were scored as follows: 0, negative staining; +, weak staining; ++, moderate staining; +++, strong staining.

DISCUSSION

Numerous studies have shown the oncogenic role of YAP in human tumors. Specifically, YAP expression was found elevated in human pancreatic cancer, liver cancer, and gastric cancer whereby YAP knockdown reduced proliferation, metastasis, and anchorage independent growth (Diep et al. 2012; Zhang et al. 2012; Liu et al. 2010a). However, recent reports have also indicated that YAP may play a tumor suppressive role (Basu et al. 2003; Zhang et al. 2012; Strano et al. 2005). YAP was shown to serve as a coactivator of p73-dependent transcription of apoptotic target gene *p53AIP1* that induces cell death in human lung carcinoma cell line and human colon carcinoma cell line, whereby silencing YAP expression reduced p73-mediated apoptosis (Strano et al. 2005). In addition, YAP protein expression was decreased or lost in breast cancers. Functionally, shRNA knockdown of YAP in breast cell lines suppressed anoikis, increased migration and invasiveness, inhibited the response to taxol, and enhanced tumor growth in nude mice (Yuan et al. 2008). Therefore the biological effects of YAP appear to vary depending on cell type and tissue context. With respect to HNSCC, greater YAP expression has been found in human HNSCC tissue samples depending on tumor grade, and was specifically localized at the tumor invasive front (Ge et al. 2011). Furthermore, amplification of chromosome region 11q22 containing the YAP gene has been identified (Overholtzer et al. 2006; Baldwin et al. 2005; Snijders et al. 2005). However, the specific biological effects of YAP in HNSCC have yet to be determined.

In this study we show that YAP plays a significant role in the growth and metastatic progression specifically in HNSCC. YAP knockdown in SCC23 cell line caused a reduction of inherent proliferative and invasive capabilities compared to control

in vitro. When subcutaneously injected into nude mice YAP knockdown decreased tumor formation and growth *in vivo*. Our *in vitro* data was also corroborated in HNSCC cell line, SCC1. Consistent with these findings, we found that the level of YAP was elevated in HNSCC compared with that of normal epithelial tissue. Moreover, YAP abundance was associated with HNSCC metastasis where greater YAP expression was seen in SCC with lymph node metastasis and SCC in lymph nodes compared to SCC without lymph nodes. Taken together, our data indicate that YAP may play an important role in HNSCC tumorigenesis and metastasis.

It will be important to confirm whether the Hippo pathway also serves as the primary negative regulator in HNSCC, because despite Hippo being the canonical mechanism by which YAP is inactivated, studies have identified alternative methods by which YAP activity in the nucleus is reduced. For example, Akt can phosphorylate YAP at Ser127 to induce interaction with 14-3-3 and attenuate its activity in a breast cancer cell line (Basu et al. 2003). More recently, Angiomotin (AMOT) family proteins, cytoplasmic proteins that can regulate cell migration and cell shape, was shown to inhibit YAP activity by physical interaction that results in either the recruitment of YAP to various compartments such as tight junctions and actin cytoskeleton independent of phosphorylation by Lats1/2, or by promoting YAP phosphorylation resulting in its degradation (Zhao et al. 2011). EBP50, a submembranous scaffolding protein, can physically bind with YAP to compartmentalize YAP at the apical membrane, leading to changes in ion transport, cytoskeletal organization, and gene expression in epithelial cells (Mohler et al. 1999). PTPN14, a non-receptor tyrosine phosphatase, was also shown to

bind and inactivate YAP by promoting nuclear exclusion by cytoplasmic retention resulting in downregulation of YAP target genes (Michaloglou et al. 2013).

Furthermore, recent findings have identified extracellular regulators of the mammalian Hippo pathway. Hippo pathway is regulated by G-protein-coupled receptor (GPCR) signaling. Serum-borne lysophosphatidic acid (LPA) and sphingosine 1-phosphophate (S1P) act through G12/13-coupled receptors to inhibit the Hippo pathway kinases Lats1/2, thereby activating YAP to induce gene expression, cell migration, and proliferation (Bin Zhao et al. 2012). In a separate study, thrombin which stimulates protease-activated receptors (PARs), another subfamily of GPCRs, was found to act through G12/13 to inhibit Lats1/2 and activating YAP to stimulate gene expression, cell migration, and cell invasion (Mo et al. 2012). In addition, the WNT pathway signaling through B-catenin could hyperactivate YAP by physically interaction with YAP and promoting its nuclear accumulation for the expression of WNT target genes (Heallen et al. 2011; Imajo et al. 2012). Considering the biological role that YAP may play based on tissue context and the alternative mechanisms by which YAP can be regulated, it will be very interesting to see specific YAP activity and response by other extracellular cues.

CHAPTER 5

YAP IS A MEDIATOR OF HGF INDUCED CANCER PROGRESSION

RESULTS

5.1 HGF Induces Scattering of HNSCC

HGF concentration in metastatic HNSCC tissues is increased compared to non-metastatic HNSCC tissues and normal gingiva. In addition, serum HGF levels correlate significantly with tumor stage progression with increased levels in advanced stage disease in HNSCC, indicating that HGF plays a crucial role in the metastatic progression of HNSCC (Hasina et al. 1999; Marshall and Kornberg 1998; Uchida et al. 2001). To determine whether HGF stimulation could induce movement and scattering of SCC23 cells, we formed cell colonies by maintaining the growth of cells starting with a low seeding concentration. Control cells without HGF treatment formed compact epithelial islands, whereas cells treated with HGF showed morphological change as early as 1 hour forming spike like projection at the edge of islands, leading to dissociation of cells exhibiting a scattered morphology by 24 hours (Fig. 5-1A). As expected, treatment of cells with HGF caused scattering of almost all colonies as opposed to no scattering in control (Fig. 5-1B).

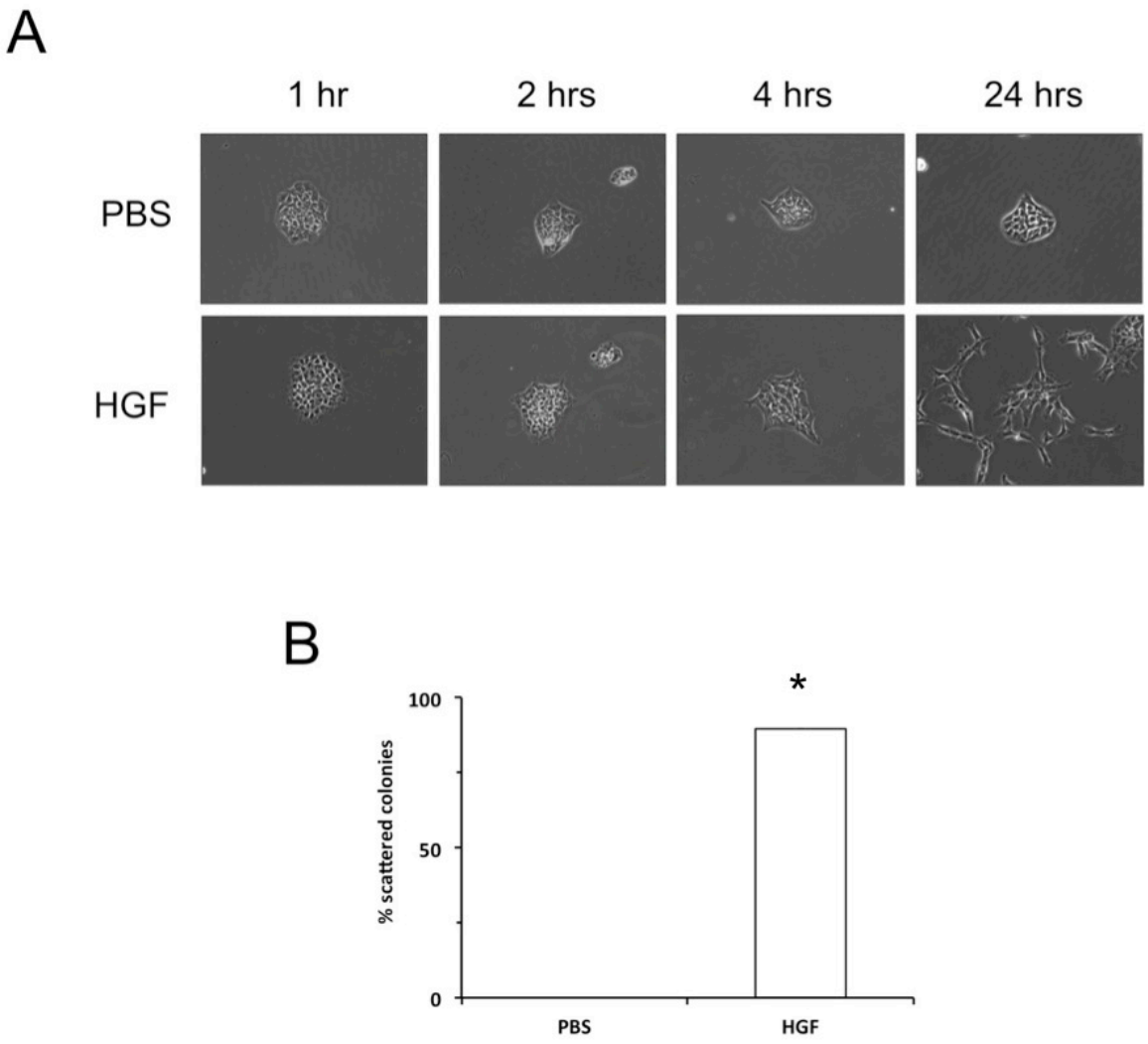

Figure 5-1. HGF induces SCC23 cell scattering. (A) Light microscopy at 20x magnification of SCC23 either untreated (PBS) or treated with HGF (20ng/mL) for 0, 1, 4, and 24 hours. (B) Bar graph quantifying scattered colonies after 24 hour HGF treatment as seen in (A). Colonies were counted at 4x magnification in three fields (n = 3). Data are means ± SD of triplicate samples from a representative experiment. *$P < 0.01$, unpaired two-tailed Student's *t* test.

5.2 YAP Knockdown Inhibits HGF Mediated Proliferation and Invasion of HNSCC

The transcriptional coactivator YAP has been identified as an oncogene that plays an important role in cancer cell proliferation and invasion (Harvey et al. 2013; Zhao et al. 2008a). YAP is the final effector of the Hippo pathway, which when activated, negatively regulates YAP by phosphorylation, leading to cytoplasmic sequestration resulting in its degradation or association with proteins to affect other signaling pathways. But despite its key role in the Hippo pathway, upstream regulation is still no clear. More recently, extracellular cues such as LPA, S1P, and Wnt have been shown to regulate YAP activity (Bin Zhao et al. 2012). Therefore we sought to discover whether YAP could play a role in the HGF mediated growth and invasion of HNSCC. To determine whether YAP was necessary for HGF mediated proliferation, we preformed MTT assay. The MTT assay is based on the conversion of water soluble MTT into insoluble formazan crystals by living cells within the mitochondria which is then dissolved in DMSO and the resulting purple solution spectrophotometrically measured. By treating YAP knockdown SCC23 cells from our previous study with HGF, our results indicate that YAP knockdown can significantly inhibit HGF mediated proliferation over the course of three days (Fig. 5-2A).

To determine whether YAP was necessary for HGF mediated cell migration, we performed cell scratch assay where confluent monolayer of cells was "scratched' by scraping a clear patch and observing the movement of cells towards the empty space. Our results show that YAP knockdown can inhibit both basal level migration and HGF mediated migration of SCC23 cells (Fig. 5-2B). Results from our invasion assay also corroborated our migration results where YAP knockdown inhibited HGF mediated

invasion (Fig. 5-2C). Taken together, our findings show that YAP may play an important role in HGF mediated proliferation and invasion of HNSCC.

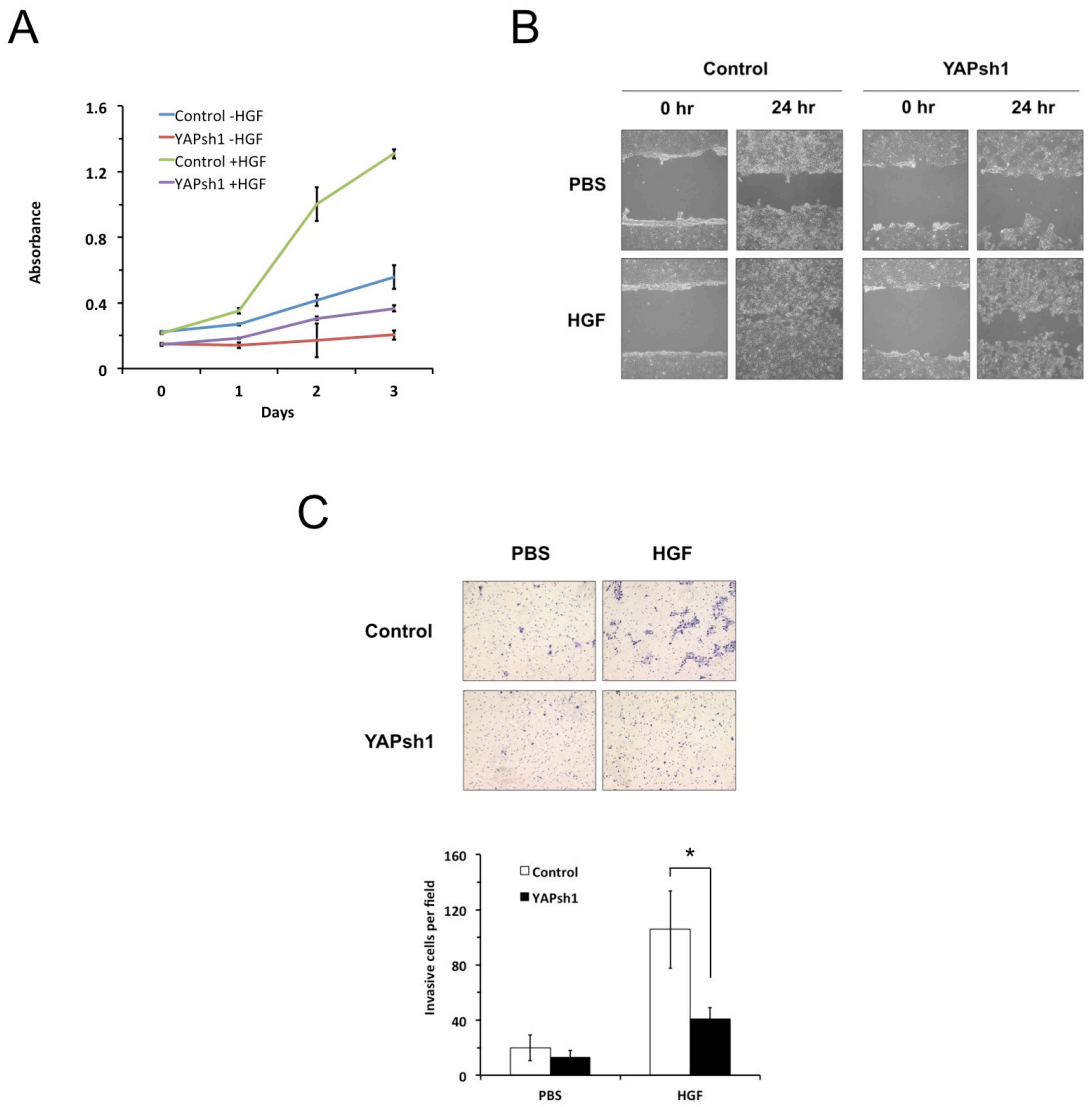

Figure 5-2. YAP knockdown inhibits HGF mediated proliferation, migration and invasion of SCC23 cells. (A) Proliferation analysis of control cells without HGF (Control −HGF), control cells with HGF (Control +HGF), YAP knockdown without HGF (YAPsh1 −HGF), and YAP knockdown with HGF (YAPsh1 +HGF), *n*=3. (B) Representative images at 4X magnification for cell migration of cells as described in (A) *n*=3. (C) Analysis of invasion using cells described in (A). (Top) Representative brightfield images. (Bottom) Data are means ± SD of triplicate samples from representative experiments (*n*=3). **P* < 0.05, unpaired two-tailed student's *t* test.

5.3 Systems Level Analysis of Transcriptional Genes Mediated by YAP in Response to HGF

To investigate how YAP can promote HGF mediated effects in HNSCC, we performed microarray analysis. By analyzing RNA expression patterns between control and YAP knockdown with or without HGF treatment, we sought to identify genes that may be important in YAP mediated invasion in response to HGF stimulation. An informative method for identifying biologically relevant patterns in high-dimensioanl microarray data sets is weighted gene co-expression network analysis (WGCNA). Analysis using WGCNA can group genes into modules that have strongly covarying patterns across multiple sample sets, which can as in our case, identify gene expression patterns related to HGF stimulation with or without YAP. Therefore by using WGCNA on our microarray data, we identified 11 distinct consensus modules (Fig. 5-3A). Modules were defined as branches of the dendrogram obtained from clustering and labeled as colors beneath the dendrogram.

To study module composition we defined the first principal component of each module as the module eigenegene (ME), which can be considered a weighted average of the probe expression profiles that make up the module. ME was then correlated to samples, e.g., control or YAP knockdown, with or without HGF stimulation. These trait specific significance measures were then correlated with module membership for each gene within a module such that a correlation coefficient, and associated *p* value, was assigned for each module and variable (Fig. 5-3B). In our attempt to identify genes that may be important in YAP mediated proliferation and invasion in response to HGF stimulation, we sought to find a specific expression pattern where genes were upregulated

in response to HGF in control, but remained low in YAP knockdown cells despite HGF treatment. The green module displayed no significant differences between samples except for the upregulation found in control cells treated with HGF. Based on our data we focused on the green module for further analysis to identify potential genes that were important in promoting growth and invasion, mediated by YAP in response to HGF stimulation.

The green module contained 2145 upregulated genes most likely to be regulated by YAP in response to HGF stimulation (Fig. 5-4A). To identify most likely candidate genes, we sorted our gene list first by greatest upregulation in control treated with HGF compared to control without HGF, followed by the least difference between YAP knockdown without HGF and control without HGF, then by the least difference between YAP knockdown with HGF and control without HGF. The resulting list ranked the top 20 genes with the greatest upregulation when treated with HGF that is most likely regulated by YAP (Table. 5-1). By far the most upregulated gene based on our ranking was matrix metalloproteinase 3 (MMP3). MMPs are proteolytic enzymes that can regulate various cell behaviors with relevance to cancer biology such as, cancer-cell growth, differentiation, apoptosis, migration, and invasion (Friedl and Gilmour 2009; Talbot et al. 2012). There activation is increased in almost all human cancers compared with normal tissue. More specifically, mouse models have shown MMP3 expression is associated with tumorigenesis and angiogenesis, and that MMP3 could induce EMT and malignant transformation in mouse mammary epithelial cells *in vitro* (NOEL et al. 2008). But despite these findings, how MMP3 expression is regulated is largely unknown. From our list we also identified the upregulation of interleukin 6 (IL6), a pro-inflammatory

cytokine that can influence all stages of tumor development including initiation, promotion, progression and metastasis. Surprisingly, our list contained additional interleukins including IL-1A, IL-8, and IL-24.

We confirmed our microarray results by performing qPCR for MMP3, IL1a, and IL6 (Fig. 5-4B). By collecting samples from 0, 1, 4, and 24 hour timepoints, we saw a gradual increase in transcription of MMP3. IL1A expression plateaued after 1 hour, but remained relatively consistent throughout the course of 24 hours. IL6 mRNA expression was upregulated approximately 3 fold compared to control, then do reduce back to basal levels at 4 hours, and increased back after 24 hours. This type of expression may be due to autoregulation of the IL6 gene resulting in a sigmoidal expression pattern. We also tested additional genes to confirm our microarray data that was not included in our green module (Fig. 5-4C). Genes KRT5, FAT2, and SMURF2 also corroborated expression change over 24 hours.

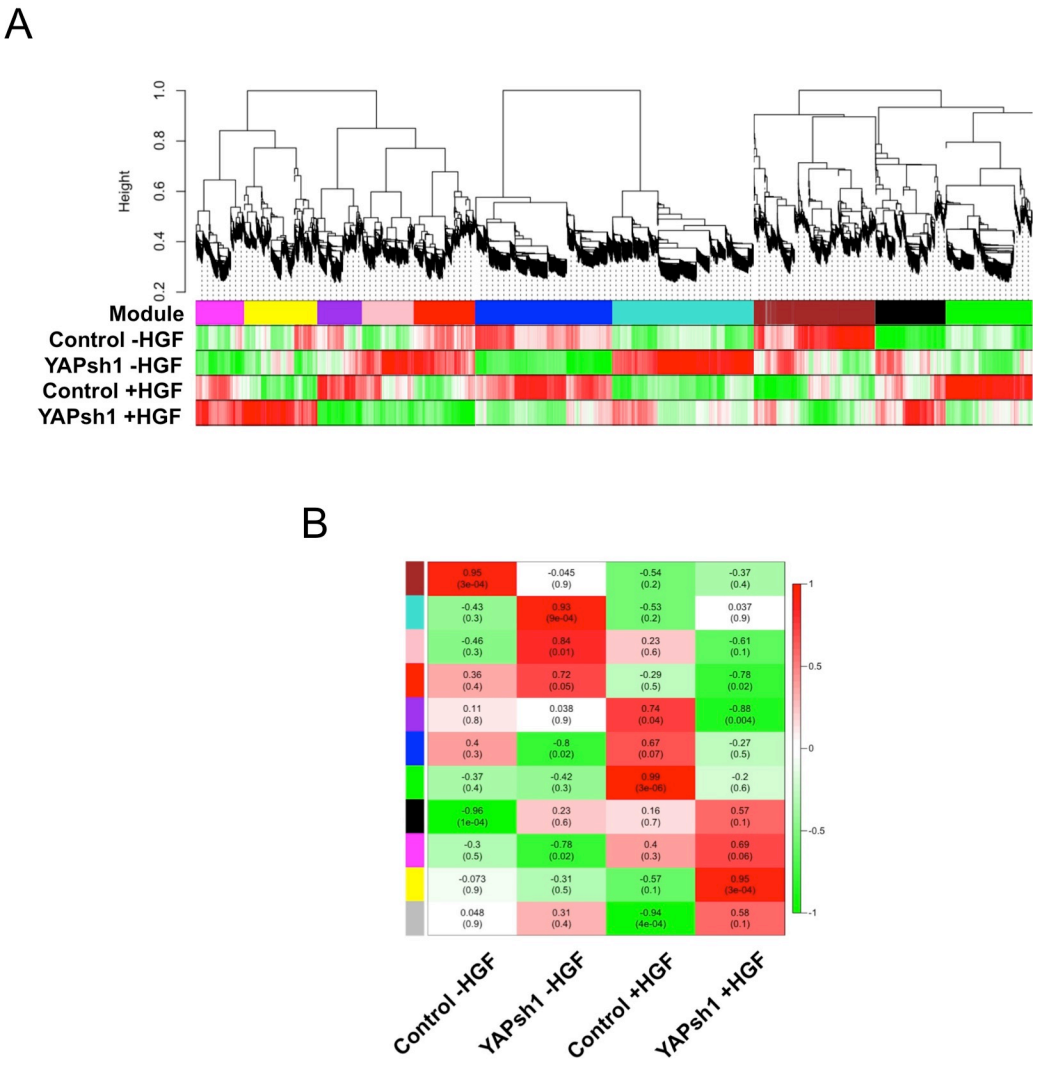

Figure 5-3. Global gene network. (A) Top: Cluster dendrogram groups genes into distinct modules using samples control without HGF (Control −HGF), YAP knockdown without HGF (YAPsh1 −HGF), control with HGF (Control +HGF), and YAP knockdown with HGF (YAPsh1 +HGF), with the *y* axis corresponding to co-expression distance between genes and the *x* axis to genes . Bottom: Top band; color coded gene modules. Bottom four bands; degree of correlation of genes among samples. Color bands indicate positive (Red), negative (Green), and no significant (White) correlation. (B) Trait relations of module network. Colors to the left represent the 11 modules from the network. For each module, the heatmap shows ME correlations to traits. Numbers in each cell report the correlation coefficients and Student asymptotic p value (parentheses) for significant ME-trait relationships. Scale bar, right, indicates the range of possible correlations from positive (red, 1) to negative (green, -1).

Accession	Definition	Gene	Control -HGF	YAPsh1 -HGF	Control +HGF	YAPsh1 +HGF
NM_002422	Homo sapiens matrix metallopeptidase 3	MMP3	89.40	116.80	2478.60	314.88
NM_002575	Homo sapiens serpin peptidase inhibitor, clade B (ovalbumin), member 2	SERPINB2	56.47	16.92	942.95	298.55
NM_001945	Homo sapiens heparin-binding EGF-like growth factor	HBEGF	113.78	65.37	677.82	314.11
NM_000584	Homo sapiens interleukin 8	IL8	183.39	167.54	981.70	256.42
NM_005118	Homo sapiens tumor necrosis factor (ligand) superfamily, member 15	TNFSF15	47.32	51.16	211.43	34.33
NM_004417	Homo sapiens dual specificity phosphatase 1	DUSP1	132.83	67.23	592.14	148.58
NM_003364	Homo sapiens uridine phosphorylase 1	UPP1	187.23	50.85	771.13	293.87
NM_014705	Homo sapiens dedicator of cytokinesis 4	DOCK4	22.71	19.98	83.72	36.89
NM_014330	Homo sapiens protein phosphatase 1, regulatory subunit 15A	PPP1R15A	136.54	89.41	466.75	147.40
NM_003236	Homo sapiens transforming growth factor, alpha	TGFA	140.16	65.18	478.22	284.36
NM_197941	Homo sapiens ADAM metallopeptidase with thrombospondin type 1 motif, 6	ADAMTS6	19.62	19.61	65.07	31.06
NM_000575	Homo sapiens interleukin 1, alpha	IL1A	443.11	36.34	1426.59	290.18
NM_006850	Homo sapiens interleukin 24	IL24	12.50	15.10	39.25	17.07
NM_031459	Homo sapiens sestrin 2	SESN2	68.11	62.43	203.72	75.40
NM_032572	Homo sapiens ribonuclease, RNase A family, 7	RNASE7	33.21	34.39	95.39	41.37
NM_003115	Homo sapiens UDP-N-acteylglucosamine pyrophosphorylase 1	UAP1	359.99	175.28	1018.90	390.02
NM_000963	Homo sapiens prostaglandin-endoperoxide synthase 2	PTGS2	25.83	18.54	73.10	29.40
NM_003447	Homo sapiens zinc finger protein 165	ZNF165	101.18	43.10	281.68	48.30
NM_000600	Homo sapiens interleukin 6	IL6	54.83	16.26	152.32	22.67
NM_002089	Homo sapiens chemokine (C-X-C motif) ligand 2	CXCL2	123.27	85.63	342.23	62.70

Table 5-1. Top 20 genes most likely regulated by YAP in response to HGF stimulation, based on the green module

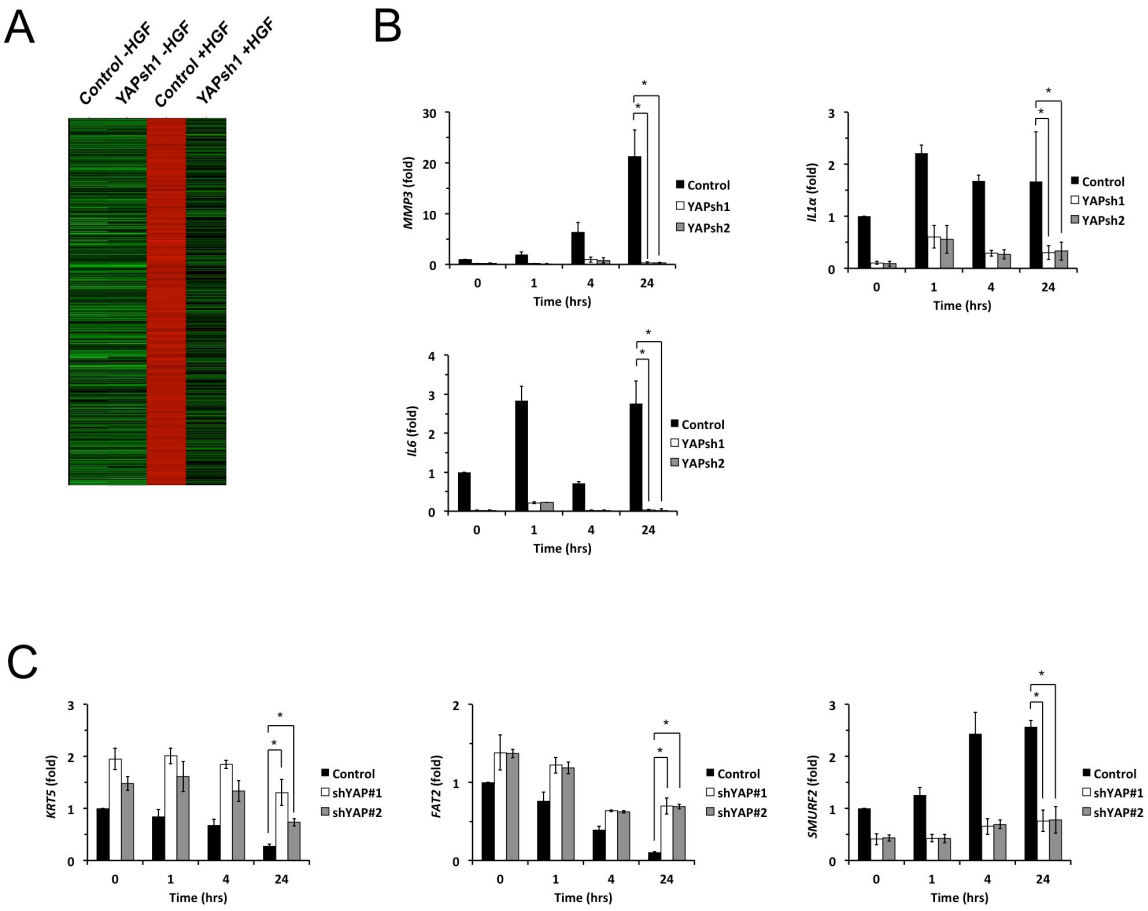

Figure 5-4. YAP knockdown inhibits HGF mediated gene expression. (A) Heatmap of green module using samples control without HGF (Control −HGF), YAP knockdown without HGF (YAPsh1 −HGF), control with HGF (Control +HGF), and YAP knockdown with HGF (YAPsh1 +HGF). Red indicates upregulation, green indicates downregulation, and black indicates no change. (B) qPCR for 0, 1, 4, and 24 hour HGF treated timepoints for select genes *MMP3*, *IL1A*, and *IL6* from Table 5-1. (C) Additional qPCR for 0, 1, 4, and 24 hour HGF treated timepoints to confirm microarray results. *p<0.01, unpaired two-tailed Student's *t* test (*n*=2)

5.4 Transcription Factor TEAD Knockdown Replicates YAP Knockdown Results

YAP is a transcriptional coactivator that does not have a DNA binding domain of its own. Instead it fulfills its primary role by binding and activating transcription factors. Several transcription factors such as ErbB4, Runx2, and p73 have been reported to bind with YAP (Li et al. 2010; Ehsanian et al. 2010). However, the TEAD family of transcription factors has been identified as the most potent YAP target for transcription activity (Lamar et al. 2012; Zhao et al. 2008b; Ota and Sasaki 2008). To determine whether TEAD was necessary for YAP mediate expression of genes in response to HGF stimulation, we created TEAD knockdown SCC23 stable cell lines using two different shRNA vectors. There are four TEAD family members (TEAD1-4). The shRNA vectors used were designed in a region identical in TEAD1, TEAD3, and TEAD4. qPCR confirmed knockdown of TEAD1, TEAD3, and TEAD4 concurrently, but not TEAD2 (Fig. 5-5A). Rather TEAD2 RNA expression levels increased, perhaps due to the cellular attempt to compensate in response to the downregulation of TEAD1, TEAD3, and TEAD4. Nevertheless, qPCR for HGF stimulation timepoints using both TEAD1/3/4 shRNAs showed similar results as in YAP knockdown for MMP3, IL1A, and IL6 from the green module(Fig. 5-5B), as well as for additional genes KRT5, FAT2, and SMURF2 (fig. 5-5C). Our results indicate that TEAD is required for YAP mediated expression of genes in response to HGF treatment in HNSCC.

TEAD is necessary for transcription of genes regulated by YAP in response to HGF stimulation. Therefore we sought to determine whether TEAD is also required for growth and invasion of HNSCC when stimulated with HGF. We performed MTT assay

over a course of three days using control and TEAD knockdown cell lines with or without HGF stimulation (Fig. 5-6A). Our results indicated that TEAD knockdown can inhibit basal and HGF stimulated proliferation in SCC23. Concurrently, TEAD knockdown also inhibited HGF mediated invasion of SCC23 (Fig. 5-6B)

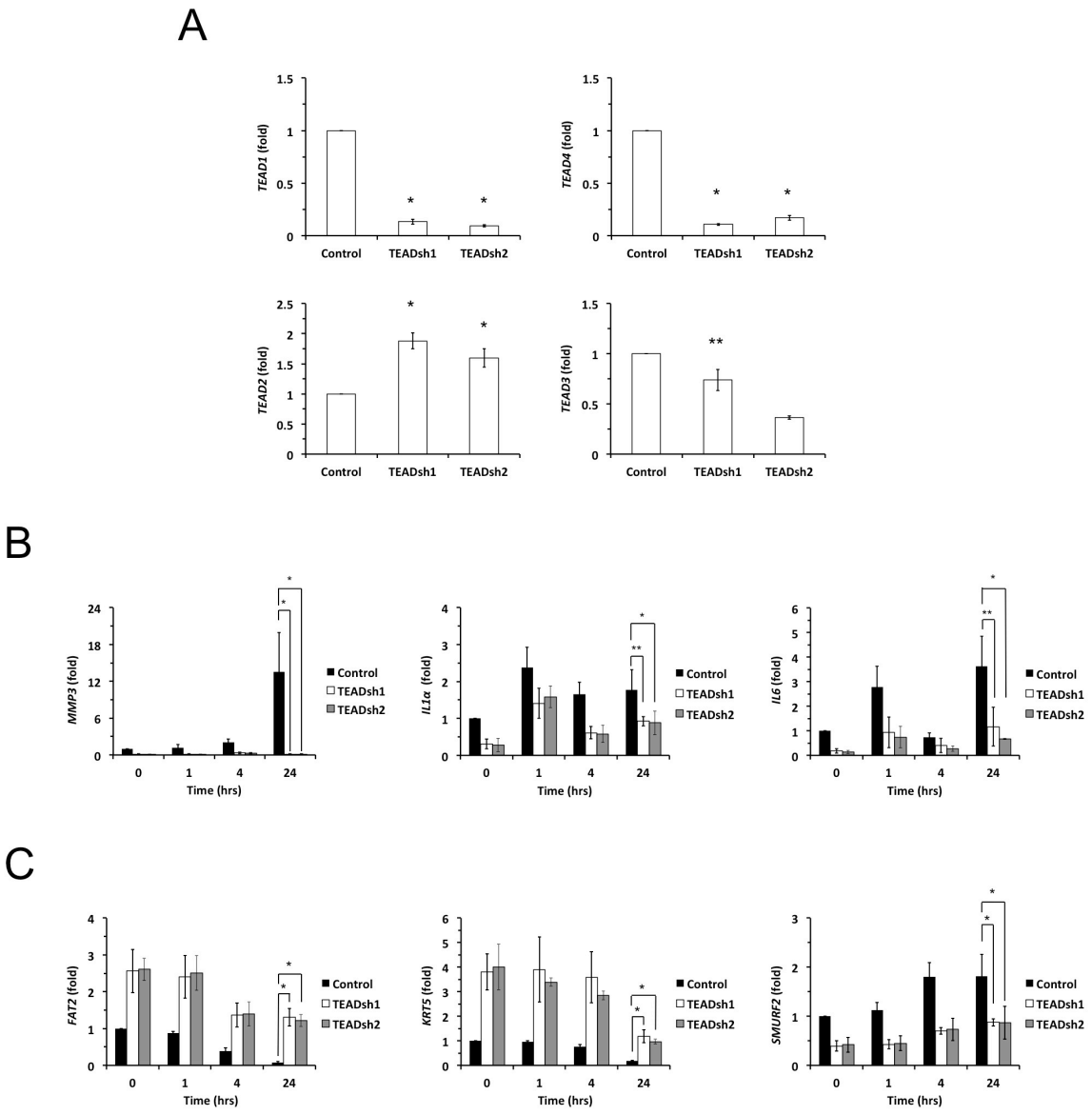

Figure 5-5. TEAD knockdown inhibits HGF mediated gene expression. (A) qPCR results confirming TEAD1/3/4 knockdown of SCC23 cells stably expressing one of two shRNA vectors targeting TEAD1, TEAD3, and TEAD4 (TEADsh1, TEADsh2). (B) qPCR for 0, 1, 4, and 24 hour HGF treated timepoints for select genes *MMP3*, *IL1A*, and *IL6* from Table XXX. (C) Additional qPCR for 0, 1, 4, and 24 hour HGF treated timepoints to confirm microarray results. *p<0.01, **p<0.05, unpaired two-tailed Student's t test (n=2)

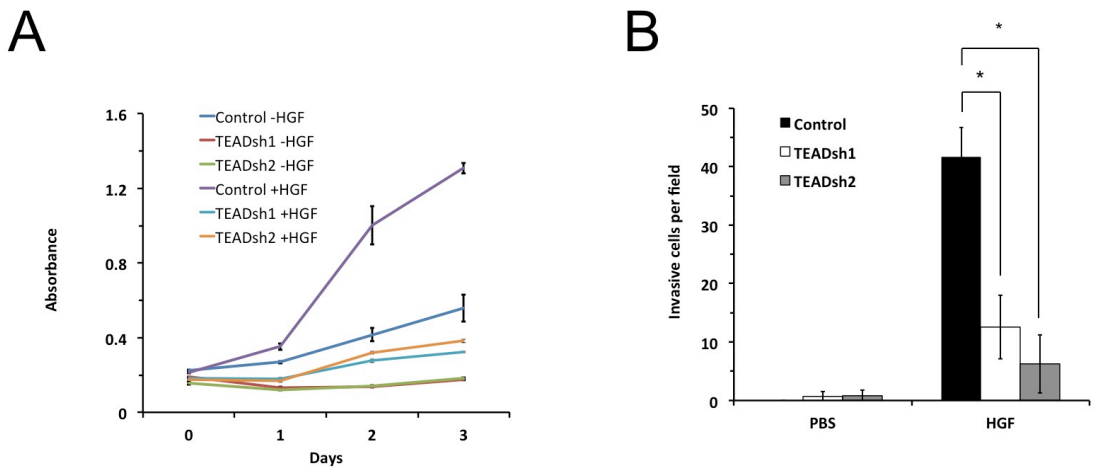

Figure 5-6. TEAD knockdown inhibits HGF mediated proliferation, migration and invasion of SCC23 cells. (A) Proliferation analysis of control cells without HGF (Control -HGF), control cells with HGF (Control +HGF), TEAD knockdown without HGF (TEADsh1 -HGF, TEADsh2 -HGF), and YAP knockdown with HGF (TEADsh1 +HGF, TEADsh2 +HGF), *n*=3. (B) Analysis of invasion using cells described in (A). Data are means ± SD of triplicate samples from representative experiments (*n*=3). **P* < 0.01, unpaired two-tailed student's *t* test.

5.5 DAVID Analysis Reveals Significant Pathways Regulated by YAP in Response to HGF

To better understand the functional significance that YAP may play in HGF mediated tumorigenesis, we further analyzed our green module using DAVID (Database for Annotation, Visualization, and Integrated Discovery). DAVID bioinformatics is a publically available tool and resource database for understanding high-level functions and utilities within a biological system especially from large datasets such as microarray. Through DAVID, we can obtain the most statistically relevant and enriched biological annotation from thousands of biological processes including molecular pathways for metabolism, genetic information processing, environmental information processing, and human disease. It serves as a useful tool that provides an overview of how differentially regulated genes may react with each other at an expression level. By using DAVID analysis, we have identified 5 pathways for which the genes from our green module is most highly associated (Table 5-2). They include the ribosome, MAPK signaling pathway, NOD-like receptor signaling pathway, Amyotrophic lateral sclerosis, and SNARE interactions in vesicular transport. We chose to focus our attention on the two pathways with greatest significance.

The ribosome pathway is the most significantly enriched annotation that also contains 25 genes from our green module (Fig. 5-7 and Table 5-3). The ribosome is large complex molecular machine comprised of more that 70 ribosomal proteins (r-proteins) that must assemble with ribosomal RNAs (rRNAs) to form the small and large ribosomal subunits 40S and 60S. The ribosome has the key role of being the central protein synthesizing machinery by translating mRNA into proteins. Our finding that the ribosome

is the most significant pathway is interesting because components of the translational machinery are deregulated or misexpressed in cancer. An up-regulated ribosome biogenesis rate could allow for, or be responsible for changes in the balance of the translational process leading to faster and more abundant protein products that may be involved in tumorigenesis (Naora et al. 1998). A variety of r-proteins having been found overexpressed in and associated with the development of malignant tumors, strongly support this idea. Select r-proteins have been identified in numerous solid tumors of the colon, lung, liver, as well as in leukemia, which often times correlates with tumor stage. Unfortunately, it is still not clear how ribosomal synthesis is deregulated (Pardee 1989).

Mitogen-activated protein kinase (MAPK) pathways are evolutionarily conserved kinase modules that link extracellular signals to machinery that control fundamental cellular processes. Specifically, MAPK pathways are comprised of a three-tier kinase module in which a MAPK is activated upon phosphorylation by a mitogen-activated protein kinase kinase (MAPKK), which in turn is activated when phosphorylated by a MAPKKK. To date there are three main MAPKs that have been characterized in mammals, extracellular signal-regulated kinase (ERK), Jun N-terminal kinase (JNK), and p38 (Frost et al. 1997; Dhillon et al. 2007; Coles and Shaw 2002). DAVID analysis revealed 43 genes from our green module that were associated with the MAPK signaling pathway (Fig. 5-8 and Table 5-4). Interestingly, we saw upregulation of genes relevant to all tiers of the MAP kinase cascade for all three fundamental MAPK pathways, ERK, JNK, and p38. Furthermore, we saw upregulation of genes upstream and downstream of the MAP kinase pathway from extracellular ligands, receptors, and transcription factors.

Term	Count	%	p-value
MAPK signaling pathway	43	2.4	6.50E-05
Ribosome	25	1.4	1.50E-07
NOD-like receptor signaling pathway	12	0.7	1.50E-02
Amyotrophic lateral sclerosis (ALS)	11	0.6	1.30E-02
SNARE interactions in vesicular transport	9	0.5	1.40E-02

Table 5-2. 5 Most significant pathway of green module analyzed through DAVID

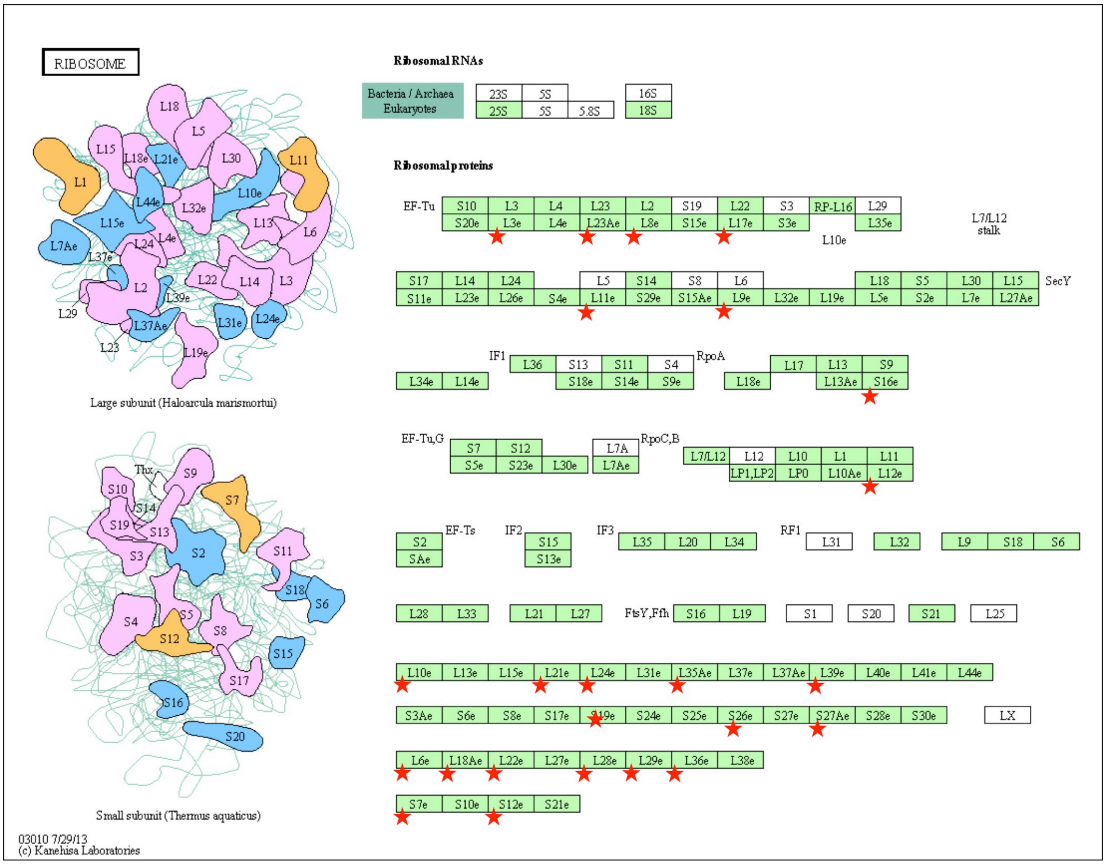

Figure 5-7. Ribosome pathway by DAVID analysis of green module. Red stars indicate genes from the green module. Refer to Table 5-3 for list of genes.

Table 5-3. Ribosome pathway gene list from green module by DAVID analysis

Official gene symbol	Complete gene name
RSL24D1P11	ribosomal L24 domain containing 1
RPL10	ribosomal protein L10
RPL11	ribosomal protein L11
RPL12	ribosomal protein L12
PRL17	ribosomal protein L17
RPL18A	ribosomal protein L18a
RPL21	ribosomal protein L21
RPL22L1	ribosomal protein L22-like 1
RPL23A	ribosomal protein L23a
RPL28	ribosomal protein L28
RPL29	ribosomal protein L29
RPL35A	ribosomal protein L35a
RPL36	ribosomal protein L36
RPL36AL	ribosomal protein L36a-like
RPL39P32	ribosomal protein L39
RPL3	ribosomal protein L3
RPL6	ribosomal protein L6
RPL8	ribosomal protein L8
RPL9	ribosomal protein L9
RPS12	ribosomal protein S12
RPS16	ribosomal protein S16
RPS19	ribosomal protein S19
RPS26	ribosomal protein S26
RPS27A	ribosomal protein S27a
RPS7	ribosomal protein S7

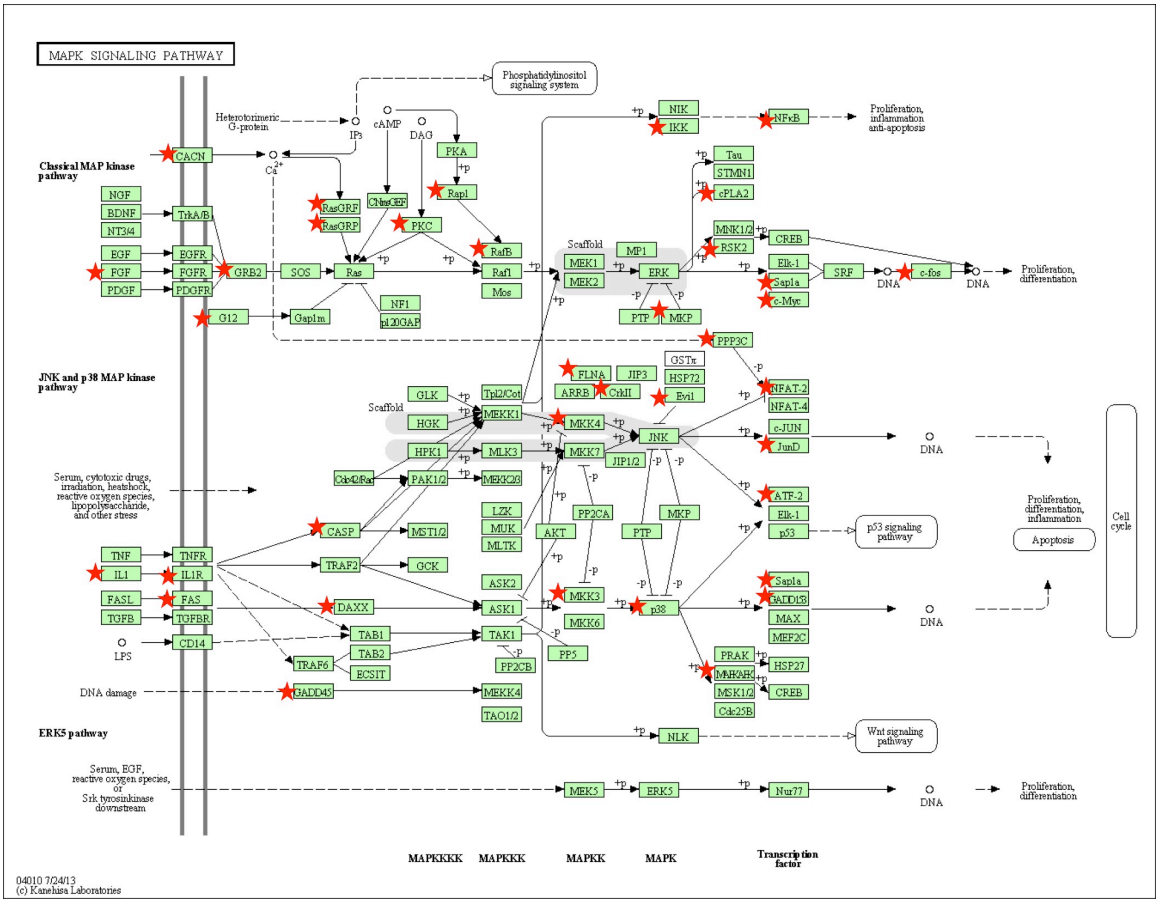

Figure 5-8. MAP kinase pathway by DAVID analysis of green module. Red stars indicate genes from the green module. Refer to Table 5-4 for list of genes.

Table 5-4. MAP kinase pathway gene list from green module by DAVID analysis

Official gene symbol	Complete gene name
Atf2	activating transcription factor 2
CACNA1S	calcium channel, voltage-dependent, L type, alpha 1S subunit
Cacna1b	calcium channel, voltage-dependent, N type, alpha 1B subunit
Casp3	caspase 3, apoptosis-related cysteine peptidase
DAXX	death-domain associated protein
DDIT3	DNA-damage-inducible transcript 3
DUSP1	dual specificity phosphatase 1
Dusp10	dual specificity phosphatase 10
DUSP16	dual specificity phosphatase 16
dusp5	dual specificity phosphatase 5
MECOM	ecotropic viral integration site 1
ELK4	ELK4, ETS-domain protein (SRF accessory protein 1)
Fas	Fas (TNF receptor superfamily, member 6)
FGF18	fibroblast growth factor 18
FLNC	filamin C, gamma (actin binding protein 280)
GADD45A	growth arrest and DNA-damage-inducible, alpha
GRB2	growth factor receptor-bound protein 2
GNG12	guanine nucleotide binding protein (G protein), gamma 12
ikbkg	inhibitor of kappa light polypeptide gene enhancer in B-cells, kinase gamma
IL1R2	interleukin 1 receptor, type II
Il1a	interleukin 1, alpha
JUND	jun D proto-oncogene
MAPK12	mitogen-activated protein kinase 12
Map2k3	mitogen-activated protein kinase kinase 3
MAP2K4	mitogen-activated protein kinase kinase 4
MAPKAPK2	mitogen-activated protein kinase-activated protein kinase 2
mapkapk3	mitogen-activated protein kinase-activated protein kinase 3
NFATC2	nuclear factor of activated T-cells,
NFKB2	nuclear factor of kappa light polypeptide gene enhancer in B-cells 2 (p49/p100)
PLA2G5	phospholipase A2, group V
Prkca	protein kinase C, alpha

PPP3CC	protein phosphatase 3 (formerly 2B), catalytic subunit, gamma isoform
RAP1A	RAP1A, member of RAS oncogene family
Rap1b	RAP1B, member of RAS oncogene family
RASGRP1	RAS guanyl releasing protein 1 (calcium and DAG-regulated)
Rasgrf2	Ras protein-specific guanine nucleotide-releasing factor 2
RRAS2	related RAS viral (r-ras) oncogene homolog 2
RPS6KA1	ribosomal protein S6 kinase, 90kDa, polypeptide 1
crk	v-crk sarcoma virus CT10 oncogene homolog (avian)
FOS	v-fos FBJ murine osteosarcoma viral oncogene homolog
MYC	v-myc myelocytomatosis viral oncogene homolog (avian)
BRAF	v-raf murine sarcoma viral oncogene homolog B1
relA	v-rel reticuloendotheliosis viral oncogene homolog A (avian)

(Table 5-4 continued)

DISCUSSION

HGF/Met activation regulates a wide array of physiological functions associated with cancer formation and metastatic progression. HGF levels in serum is often found elevated and correlates with tumor stage progression in HNSCC (Kim et al. 2007). HGF concentration in metastatic HNSCC tissues is also significantly higher that non-metastatic cancer tissues and normal gingiva (Marshall and Kornberg 1998; Uchida et al. 2001). Furthermore *in vivo* and *in vitro* studies have found HGF was able to stimulate growth and invasion of HNSCC (Kim et al. 2010). Such effects are the result of gene expression changes mediated by the regulation of numerous different signaling pathways. YAP is a transcription coactivator and its activation may therefore play an important role in HGF mediated gene regulation. Consistent with this idea are more recent findings where YAP acts as a mediator for extracellular cues such as LPA, S1P, and Wnt through G-protein-coupled receptors (GPCRs) (Bin Zhao et al. 2012). In this study, we have identified YAP along with its primary associated transcription factor TEAD to be important mediators for HGF induced gene expression change and cancer growth and invasion.

YAP knockdown was able to significantly inhibit SCC23 proliferation, migration and invasion in response to HGF stimulation. However molecular studies are necessary for understanding the details of YAP function in the context of HGF. Therefore we performed microarray analysis and by using WGCNA we identified 11 distinct coexpression modules. We focused our study on the green module because it most closely represented the set of genes positively regulated by YAP in response to HGF stimulation. The green module contained 1954 genes, which we ranked by the greatest expression difference between control with HGF and control without HGF, followed by

the least expression difference between YAP knockdown without HGF and control without HGF, as well as YAP knockdown with HGF and control without HGF in order to identify most significant genes. By far the most significant gene identified was MMP3 for which expression change was confirmed by qPCR. In addition, among the top 20 in our list, were interleukins, several of which we also confirmed by qPCR. Since TEAD is the most prominent transcription factor target for YAP, we also determined whether TEAD is necessary for gene expression changes mediated by YAP in response to HGF stimulation. qPCR results as well as proliferation and invasion results using TEAD knockdown stable cell lines treated with HGF were consistent with our data using YAP knockdown cells.

Further analysis of our green module by DAVID analysis provided interesting results, where the production of ribosome pathway showed greatest association with our gene list from the green module. Cell growth and proliferation are associated with changes in the rate of ribosome production. During G1, an increase in rRNA and ribosome assembly is a prerequisite for increased protein synthesis during S phase (Pardee 1989). Considering that HGF can mediate proliferation *in vitro* and *in vivo* (Borowiak et al. 2004; Rubin et al. 1991) in conjunction with the fact that YAP plays an vital role in proliferation and organ size control, it is possible that HGF can serve as an extracellular cue that can activate YAP for the expression r-proteins necessary for proliferation. Moreover research has shown that the overexpression of even a single r-protein such as S3a can induce transformation of NIH3T3 cells and induce formation of tumors in nude mice (Naora et al. 1998). Our analysis has identified the 25 specific r-proteins upregulated via YAP in response to HGF which can serve as an initial starting

point for further study to determine cross-talk with ribosomes and proliferation which still remains largely unknown.

The ERK pathway is perhaps the most studied among the mammalian MAPK pathways, and is deregulated in approximately one-third of all human cancers (Dhillon et al. 2007). Active ERK phosphorylates numerous cytoplasmic and nuclear targets, including kinases, phosphatases, transcription factors and cytoskeletal proteins. As a result, ERK signaling can regulate processes such as proliferation, differentiation, survival, and migration (Frost et al. 1997; Coles and Shaw 2002). Furthermore HGF/MET activation has been found to activate ERK, JNK, and p38 MAP kinase pathways to promote cancer progression (Rodrigues et al. 1997; Recio and Merlino 2002; Lamorte et al. 2000). Although these MAP kinase pathways can be activated in response to HGF, it would be interesting to see if YAP can provide another level of transcriptional control for the regulation of MAP kinase activity. Our results indicate that this may be the case.

REFERENCES

Ang KK, Harris J, Wheeler R, Weber R, Rosenthal DI, Nguyen-Tân PF, Westra WH, Chung CH, Jordan RC, Lu C, et al. 2010. Human papillomavirus and survival of patients with oropharyngeal cancer. *N Engl J Med* **363**: 24–35.

Argiris A, Karamouzis MV, Raben D, Ferris RL. 2008. Head and neck cancer. *The Lancet* **371**: 1695–1709.

Baldwin C, Garnis C, Zhang L, Rosin MP, Lam WL. 2005. Multiple microalterations detected at high frequency in oral cancer. *Cancer Research* **65**: 7561–7567.

Bardelli A, Longati P, Gramaglia D, Stella MC, Comoglio PM. 1997. Gab1 coupling to the HGF/Met receptor multifunctional docking site requires binding of Grb2 and correlates with the transforming potential. *Oncogene* **15**: 3103–3111.

Basu S, Totty NF, Irwin MS, Sudol M, Downward J. 2003. Akt phosphorylates the Yes-associated protein, YAP, to induce interaction with 14-3-3 and attenuation of p73-mediated apoptosis. *Molecular Cell* **11**: 11–23.

Bin Zhao, Lei Q-Y, Guan K-L. 2009. Harness the Power: New Insights into the Inhibition of YAP/ Yorkie. *Developmental Cell* **16**: 321–322.

Bin Zhao, Panupinthu N, Jewell JL, Lian I, Wang LH, Zhao J, Yuan H, Tumaneng K, Li H, Fu X-D, et al. 2012. Regulation of the Hippo-YAP Pathway by G-Protein-Coupled Receptor Signaling. *Cell* 1–12.

Blot WJ, McLaughlin JK, Winn DM, Austin DF, Greenberg RS, Preston-Martin S, Bernstein L, Schoenberg JB, Stemhagen A, Fraumeni JF. 1988. Smoking and drinking in relation to oral and pharyngeal cancer. *Cancer Research* **48**: 3282–3287.

Bogenrieder T, Herlyn M. 2003. Axis of evil: molecular mechanisms of cancer metastasis. *Oncogene* **22**: 6524–6536.

Borowiak M, Garratt AN, Wüstefeld T, Strehle M, Trautwein C, Birchmeier C. 2004. Met provides essential signals for liver regeneration. *Proc Natl Acad Sci USA* **101**: 10608–10613.

Bose P, Brockton NT, Dort JC. 2013. Head and neck cancer: from anatomy to biology. *Int J Cancer* n/a–n/a.

Calhoun KH, Fulmer P, Weiss R, Hokanson JA. 1994. Distant metastases from head and neck squamous cell carcinomas. *Laryngoscope* **104**: 1199–1205.

Camargo FD, Gokhale S, Johnnidis JB, Fu D, Bell GW, Jaenisch R, Brummelkamp TR. 2007. YAP1 Increases Organ Size and Expands Undifferentiated Progenitor Cells. *Current Biology* **17**: 2054–2060.

Coles LC, Shaw PE. 2002. PAK1 primes MEK1 for phosphorylation by Raf-1 kinase during cross-cascade activation of the ERK pathway. *Oncogene* **21**: 2236–2244.

D'Souza G, Kreimer AR, Viscidi R, Pawlita M, Fakhry C, Koch WM, Westra WH, Gillison ML. 2007. Case-control study of human papillomavirus and oropharyngeal cancer. *N Engl J Med* **356**: 1944–1956.

de Bree R, Haigentz M Jr, Silver CE, Paccagnella D, Hamoir M, Hartl DM, Machiels J-P, Paleri V, Rinaldo A, Shaha AR, et al. 2012. Distant metastases from head and neck squamous cell carcinoma. Part II. Diagnosis. *Oral Oncology* **48**: 780–786.

Dhillon AS, Hagan S, Rath O, Kolch W. 2007. MAP kinase signalling pathways in cancer. *Oncogene* **26**: 3279–3290.

Diep CH, Zucker KM, Hostetter G, Watanabe A, Hu C, Munoz RM, Hoff Von DD, Han H. 2012. Down-regulation of Yes Associated Protein 1 expression reduces cell proliferation and clonogenicity of pancreatic cancer cells. *PLoS ONE* **7**: e32783.

Dong J, Feldmann G, Huang J, Wu S, Zhang N, Comerford SA, Gayyed MF, Anders RA, Maitra A, Pan D. 2007. Elucidation of a Universal Size-Control Mechanism in Drosophila and Mammals. *Cell* **130**: 1120–1133.

Ehsanian R, Brown M, Lu H, Yang XP, Pattatheyil A, Yan B, Duggal P, Chuang R, Doondeea J, Feller S, et al. 2010. Oncogene_2010_Ehsanian. **29**: 6160–6171.

Fidler IJI. 2003. *The pathogenesis of cancer metastasis: the "seed and soil" hypothesis revisited.*

Foulkes WD, Brunet JS, Sieh W, Black MJ, Shenouda G, Narod SA. 1996. Familial risks of squamous cell carcinoma of the head and neck: retrospective case-control study. *BMJ* **313**: 716–721.

Friedl P, Gilmour D. 2009. nrm2720. 1–13.

Frost JA, Steen H, Shapiro P, Lewis T, Ahn N, Shaw PE, Cobb MH. 1997. Cross-cascade activation of ERKs and ternary complex factors by Rho family proteins. *EMBO J* **16**: 6426–6438.

Gao CF, Vande Woude GF. 2005. HGF/SF-Met signaling in tumor progression. *Cell Res* **15**: 49–51.

Ge L, Smail M, Meng W, Shyr Y, Ye F, Fan K-H, Li X, Zhou H-M, Bhowmick NA. 2011. Yes-Associated Protein Expression in Head and Neck Squamous Cell Carcinoma Nodal Metastasis ed. T. Ramqvist. *PLoS ONE* **6**: e27529.

Gillison ML, D'Souza G, Westra W, Sugar E, Xiao W, Begum S, Viscidi R. 2008. Distinct risk factor profiles for human papillomavirus type 16-positive and human papillomavirus type 16-negative head and neck cancers. *J Natl Cancer Inst* **100**: 407–420.

Gupta GP, Massagué J. 2006. Cancer Metastasis: Building a Framework. *Cell* **127**: 679–695.

Hanahan D, Weinberg RA. 2011. Hallmarks of Cancer: The Next Generation. *Cell* **144**: 646–674.

Hanzawa M, Shindoh M, Higashino F, Yasuda M, Inoue N, Hida K, Ono M, Kohgo T, Nakamura M, Notani K, et al. 2000. Hepatocyte growth factor upregulates E1AF that induces oral squamous cell carcinoma cell invasion by activating matrix metalloproteinase genes. *Carcinogenesis* **21**: 1079–1085.

Harvey KF, Zhang X, Thomas DM. 2013. The Hippo pathway and human cancer. **13**: 246–257. http://eutils.ncbi.nlm.nih.gov/entrez/eutils/elink.fcgi?dbfrom=pubmed&id=23467301&retmode=ref&cmd=prlinks.

Hashibe M, Boffetta P, Zaridze D, Shangina O, Szeszenia-Dabrowska N, Mates D, Janout V, Fabiánová E, Bencko V, Moullan N, et al. 2006. Evidence for an important role of alcohol- and aldehyde-metabolizing genes in cancers of the upper aerodigestive tract. *Cancer Epidemiol Biomarkers Prev* **15**: 696–703.

Hashibe M, Brennan P, Benhamou S, Castellsague X, Chen C, Curado MP, Dal Maso L, Daudt AW, Fabiánová E, Fernandez L, et al. 2007. Alcohol drinking in never users of tobacco, cigarette smoking in never drinkers, and the risk of head and neck cancer: pooled analysis in the International Head and Neck Cancer Epidemiology Consortium. *J Natl Cancer Inst* **99**: 777–789.

Hasina R, Matsumoto K, Matsumoto-Taniura N, Kato I, Sakuda M, Nakamura T. 1999. Autocrine and paracrine motility factors and their involvement in invasiveness in a human oral carcinoma cell line. *Br J Cancer* **80**: 1708–1717.

Heallen T, Zhang M, Wang J, Bonilla-Claudio M, Klysik E, Johnson RL, Martin JF. 2011. Hippo Pathway Inhibits Wnt Signaling to Restrain Cardiomyocyte Proliferation and Heart Size. *Science* **332**: 458–461.

Hida K, Shindoh M, Yasuda M, Hanzawa M, Funaoka K, Kohgo T, Amemiya A, Totsuka Y, Yoshida K, Fujinaga K. 1997. Antisense E1AF transfection restrains oral cancer invasion by reducing matrix metalloproteinase activities. *The American Journal of Pathology* **150**: 2125–2132.

Huang D. 2008. Crosstalk between tumor cells and microenvironment via Wnt pathway in colorectal cancer dissemination. *WJG* **14**: 1823.

Huber GF, Züllig L, Soltermann A, Roessle M, Graf N, Haerle SK, Studer G, Jochum W, Moch H, Stoeckli SJ. 2011. Down regulation of E-Cadherin (ECAD) - a predictor for occult metastatic disease in sentinel node biopsy of early squamous cell carcinomas of the oral cavity and oropharynx. *BMC Cancer* **11**: 217:1–8.

Imajo M, Miyatake K, Iimura A, Miyamoto A, Nishida E. 2012. A molecular mechanism that links Hippo signalling to the inhibition of Wnt/β-catenin signalling. *EMBO J* **31**: 1109–1122.

Jemal A, Siegel R, Ward E, Hao Y, Xu J, Thun MJ. 2009. Cancer Statistics, 2009. *CA: A Cancer Journal for Clinicians* **59**: 225–249.

Jiang Z, Li X, Hu J, Zhou W, Jiang Y, Li G, Lu D. 2006. Promoter hypermethylation-mediated down-regulation of LATS1 and LATS2 in human astrocytoma. *Neurosci Res* **56**: 450–458.

Jinnin M. 2005. Matrix metalloproteinase-1 up-regulation by hepatocyte growth factor in human dermal fibroblasts via ERK signaling pathway involves Ets1 and Fli1. *Nucleic Acids Research* **33**: 3540–3549.

John MAMS, Tao WW, Fei XX, Fukumoto RR, Carcangiu MLM, Brownstein DGD, Parlow AFA, McGrath JJ, Xu TT. 1999. Mice deficient of Lats1 develop soft-tissue sarcomas, ovarian tumours and pituitary dysfunction. *Nat Genet* **21**: 182–186.

Kim C-H, Koh YW, Han JH, Kim JW, Lee JS, Baek SJ, Hwang HS, Choi EC. 2010. c-Met expression as an indicator of survival outcome in patients with oral tongue carcinoma. *Head Neck* **32**: 1655–1664.

Kim C-H, Lee JS, Kang S-O, Bae J-H, Hong SP, Kahng H. 2007. Serum hepatocyte growth factor as a marker of tumor activity in head and neck squamous cell carcinoma. *Oral Oncology* **43**: 1021–1025.

Lai Z-C, Wei X, Shimizu T, Ramos E, Rohrbaugh M, Nikolaidis N, Ho L-L, Li Y. 2005. Control of cell proliferation and apoptosis by mob as tumor suppressor, mats. *Cell* **120**: 675–685.

Lamar JM, Stern P, Liu H, Schindler JW, Jiang ZG, Hynes RO. 2012. PNAS Plus: The Hippo pathway target, YAP, promotes metastasis through its TEAD-interaction domain. *Proc Natl Acad Sci USA* **109**: E2441–E2450.

Lamorte L, Kamikura DM, Park M. 2000. A switch from p130Cas/Crk to Gab1/Crk signaling correlates with anchorage independent growth and JNK activation in cells transformed by the Met receptor oncoprotein. *Oncogene* **19**: 5973–5981.

Langfelder P, Horvath S. 2008. WGCNA: an R package for weighted correlation network analysis. *BMC Bioinformatics* **9**: 559.

Lee J-H, Kim T-S, Yang T-H, Koo B-K, Oh S-P, Lee K-P, Oh H-J, Lee S-H, Kong Y-Y, Kim J-M, et al. 2008. A crucial role of WW45 in developing epithelial tissues in the mouse. *EMBO J* **27**: 1231–1242.

Leemans CR, Braakhuis BJM, Brakenhoff RH. 2010. Nat._Rev._Cancer_2011_Leemans. *Nature Publishing Group* **11**: 9–22.

Leemans CRC, Tiwari RR, Nauta JJJ, van der Waal II, Snow GBG. 1993. Regional lymph node involvement and its significance in the development of distant metastases in head and neck carcinoma. *Cancer* **71**: 452–456.

Li Z, Zhao B, Wang P, Chen F, Dong Z, Yang H, Guan KL, Xu Y. 2010. Structural insights into the YAP and TEAD complex. *Genes Dev* **24**: 235–240.

Liu AM, Wong K-F, Jiang X, Qiao Y, Luk JM. 2012. Regulators of mammalian Hippo pathway in cancer. *BBA - Reviews on Cancer* **1826**: 357–364.

Liu AM, Xu MZ, Chen J, Poon RT, Luk JM. 2010a. Targeting YAP and Hippo signaling pathway in liver cancer. *Expert Opin Ther Targets* **14**: 855–868.

Liu Y, Xin Y, Ye F, Wang W, Lu Q, Kaplan HJ, Dean DC. 2010b. Taz-tead1 links cell-cell contact to zeb1 expression, proliferation, and dedifferentiation in retinal pigment epithelial cells. *Invest Ophthalmol Vis Sci* **51**: 3372–3378.

Longati P, Bardelli A, Ponzetto C, Naldini L, Comoglio PM. 1994. Tyrosines1234-1235 are critical for activation of the tyrosine kinase encoded by the MET proto-oncogene (HGF receptor). *Oncogene* **9**: 49–57.

Marshall DD, Kornberg LJ. 1998. Overexpression of scatter factor and its receptor (c-met) in oral squamous cell carcinoma. *Laryngoscope* **108**: 1413–1417.

MD AAS, MBB MFG, PhD APK, PhD JD, MBBS AM, PhD DP, MD EAM, PhD RAAM. 2008. Expression of Yes-associated protein in common solid tumors. *Human Pathology* 1–8.

Mhawech P, Dulguerov P, Assaly M, Ares C, Allal AS. 2005. EB-D fibronectin expression in squamous cell carcinoma of the head and neck. *Oral Oncology* **41**: 82–88.

Michaloglou C, Lehmann W, Martin T, Delaunay C, Hueber A, Barys L, Niu H, Billy E, Wartmann M, Ito M, et al. 2013. The Tyrosine Phosphatase PTPN14 Is a Negative Regulator of YAP Activity ed. L.R. Languino. *PLoS ONE* **8**: e61916.

Mo JS, Yu FX, Gong R, Brown JH, Guan KL. 2012. Regulation of the Hippo-YAP pathway by protease-activated receptors (PARs). *Genes Dev* **26**: 2138–2143.

Mohler PJ, Kreda SM, Boucher RC, Sudol M, Stutts MJ, Milgram SL. 1999. Yes-associated protein 65 localizes p62(c-Yes) to the apical compartment of airway epithelia by association with EBP50. *The Journal of Cell Biology* **147**: 879–890.

Monvoisin A, Bisson C, Si-Tayeb K, Balabaud C, Desmoulière A, Rosenbaum J. 2002. Involvement of matrix metalloproteinase type-3 in hepatocyte growth factor-induced invasion of human hepatocellular carcinoma cells. *Int J Cancer* **97**: 157–162.

Nabeshima K, Inoue T, Shimao Y, Okada Y, Itoh Y, Seiki M, Koono M. 2000. Front-cell-specific expression of membrane-type 1 matrix metalloproteinase and gelatinase A during cohort migration of colon carcinoma cells induced by hepatocyte growth factor/scatter factor. *Cancer Research* **60**: 3364–3369.

Naora H, Takai I, Adachi M, Naora H. 1998. Altered cellular responses by varying expression of a ribosomal protein gene: sequential coordination of enhancement and suppression of ribosomal protein S3a gene expression induces apoptosis. *The Journal of Cell Biology* **141**: 741–753.

Nguyen PT, Kudo Y, Yoshida M, Kamata N, Ogawa I, Takata T. 2011. N-cadherin expression is involved in malignant behavior of head and neck cancer in relation to epithelial-mesenchymal transition. *Histol Histopathol* **26**: 147–156.

Noel A, Jost M, Maquoi E. 2008. Matrix metalloproteinases at cancer tumor–host interface. *Semin Cell Dev Biol* **19**: 52–60.

Ota M, Sasaki H. 2008. Mammalian Tead proteins regulate cell proliferation and contact inhibition as transcriptional mediators of Hippo signaling. *Development* **135**: 4059–4069.

Overholtzer M, Zhang J, Smolen GA, Muir B, Li W, Sgroi DC, Deng C-X, Brugge JS, Haber DA. 2006. Transforming properties of YAP, a candidate oncogene on the chromosome 11q22 amplicon. *Proc Natl Acad Sci USA* **103**: 12405–12410.

Paccione RJ, Miyazaki H, Patel V, Waseem A, Gutkind JS, Zehner ZE, Yeudall WA. 2008. Keratin down-regulation in vimentin-positive cancer cells is reversible by vimentin RNA interference, which inhibits growth and motility. *Mol Cancer Ther* **7**: 2894–2903.

Pardee AB. 1989. G1 events and regulation of cell proliferation. *Science* **246**: 603–608.

Paumelle R, Tulasne D, Kherrouche Z, Plaza S, Leroy C, Reveneau S, Vandenbunder B, Fafeur V, Tulashe D, Reveneau S. 2002. Hepatocyte growth factor/scatter factor activates the ETS1 transcription factor by a RAS-RAF-MEK-ERK signaling pathway. *Oncogene* **21**: 2309–2319.

Pelicci G, Giordano S, Zhen Z, Salcini AE, Lanfrancone L, Bardelli A, Panayotou G, Waterfield MD, Ponzetto C, Pelicci PG. 1995. The motogenic and mitogenic responses to HGF are amplified by the Shc adaptor protein. *Oncogene* **10**: 1631–1638.

Pelucchi C, Gallus S, Garavello W, Bosetti C, La Vecchia C. 2008. Alcohol and tobacco use, and cancer risk for upper aerodigestive tract and liver. *Eur J Cancer Prev* **17**: 340–344.

Recio JA, Merlino G. 2002. Hepatocyte growth factor/scatter factor activates proliferation in melanoma cells through p38 MAPK, ATF-2 and cyclin D1. *Oncogene* **21**: 1000–1008.

Rodrigues GA, Park M, Schlessinger J. 1997. Activation of the JNK pathway is essential for transformation by the Met oncogene. *EMBO J* **16**: 2634–2645.

Rosenthal EL, Johnson TM, Allen ED, Apel IJ, Punturieri A, Weiss SJ. 1998. Role of the plasminogen activator and matrix metalloproteinase systems in epidermal growth factor- and scatter factor-stimulated invasion of carcinoma cells. *Cancer Research* **58**: 5221–5230.

Rubin JS, Chan AM, Bottaro DP, Burgess WH, Taylor WG, Cech AC, Hirschfield DW, Wong J, Miki T, Finch PW. 1991. A broad-spectrum human lung fibroblast-derived mitogen is a variant of hepatocyte growth factor. *Proc Natl Acad Sci USA* **88**: 415–419.

Saman Warnakulasuriya. 2009. Global epidemiology of oral and oropharyngeal cancer. *Oral Oncology* **45**: 309–316.

Sano D, Myers JN. 2007. Metastasis of squamous cell carcinoma of the oral tongue. *Cancer Metastasis Rev* **26**: 645–662.

Scanlon CS, Van Tubergen EA, Inglehart RC, D'Silva NJ. 2013. Biomarkers of Epithelial-Mesenchymal Transition in Squamous Cell Carcinoma. *Journal of Dental Research* **92**: 114–121.

Schlecht NF, Franco EL, Pintos J, Kowalski LP. 1999. Effect of smoking cessation and tobacco type on the risk of cancers of the upper aero-digestive tract in Brazil. *Epidemiology* **10**: 412–418.

Snijders AM, Schmidt BL, Fridlyand J, Dekker N, Pinkel D, Jordan RCK, Albertson DG. 2005. Rare amplicons implicate frequent deregulation of cell fate specification pathways in oral squamous cell carcinoma. *Oncogene* **24**: 4232–4242.

Strano S, Monti O, Pediconi N, Baccarini A, Fontemaggi G, Lapi E, Mantovani F, Damalas A, Citro G, Sacchi A. 2005. The Transcriptional Coactivator Yes-Associated Protein Drives p73 Gene-Target Specificity in Response to DNA Damage. *Molecular Cell* **18**: 447–459.

Sturgis EM, Cinciripini PM. 2007. Trends in head and neck cancer incidence in relation to smoking prevalence: an emerging epidemic of human papillomavirus-associated cancers? *Cancer* **110**: 1429–1435.

Sturgis EM, Dahlstrom KR, Spitz MR, Wei Q. 2002. DNA repair gene ERCC1 and ERCC2/XPD polymorphisms and risk of squamous cell carcinoma of the head and neck. *Arch Otolaryngol Head Neck Surg* **128**: 1084–1088.

Suárez C, Rodrigo JP, Ferlito A, Cabanillas R, Shaha AR, Rinaldo A. 2006. Tumours of familial origin in the head and neck. *Oral Oncology* **42**: 965–978.

Talbot LJ, Bhattacharya SD, Kuo PC. 2012. Epithelial-mesenchymal transition, the tumor microenvironment, and metastatic behavior of epithelial malignancies. *Int J Biochem Mol Biol* **3**: 117–136.

Tapon N, Harvey KF, Bell DW, Wahrer DCR, Schiripo TA, Haber DA, Hariharan IK. 2002. salvador Promotes both cell cycle exit and apoptosis in Drosophila and is mutated in human cancer cell lines. *Cell* **110**: 467–478.

Trizna Z, Schantz SP. 1992. Hereditary and environmental factors associated with risk and progression of head and neck cancer. *Otolaryngol Clin North Am* **25**: 1089–1103.

Trusolino L, Comoglio PM. 2002. SCATTER-FACTOR AND SEMAPHORIN RECEPTORS: CELL SIGNALLING FOR INVASIVE GROWTH. *Nat Rev Cancer* **2**: 289–300.

Uchida D, Kawamata H, Omotehara F, Nakashiro Ki, Kimura-Yanagawa T, Hino S, Begum NM, Hoque MO, Yoshida H, Sato M, et al. 2001. Role of HGF/c-met system in invasion and metastasis of oral squamous cell carcinoma cells in vitro and its clinical significance. *Int J Cancer* **93**: 489–496.

Weidner KM, Di Cesare S, Sachs M, Brinkmann V, Behrens J, Birchmeier W. 1996. Interaction between Gab1 and the c-Met receptor tyrosine kinase is responsible for epithelial morphogenesis. *Nature* **384**: 173–176.

Wheelock MJ, Johnson KR. 2003. Cadherin-mediated cellular signaling. *Current Opinion in Cell Biology* **15**: 509–514.

Wu H, Lotan R, Menter D, Lippman SM, Xu XC. 2000. Expression of E-cadherin is associated with squamous differentiation in squamous cell carcinomas. *Anticancer Res* **20**: 1385–1390.

Yoon Y, Liang Z, Zhang X, Choe M, Zhu A, Cho HT, Shin DM, Goodman MM, Chen ZG, Shim H. 2007. CXC chemokine receptor-4 antagonist blocks both growth of primary tumor and metastasis of head and neck cancer in xenograft mouse models. *Cancer Research* **67**: 7518–7524.

Yuan M, Tomlinson V, Lara R, Holliday D, Chelala C, Harada T, Gangeswaran R, Manson-Bishop C, Smith P, Danovi SA, et al. 2008. Yes-associated protein (YAP) functions as a tumor suppressor in breast. *Cell Death Differ* **15**: 1752–1759.

Zeisberg M, Neilson EG. 2009. Biomarkers for epithelial-mesenchymal transitions. *J Clin Invest* **119**: 1429–1437.

Zender L, Spector MS, Xue W, Flemming P, Cordon-Cardo C, Silke J, Fan S-T, Luk JM, Wigler M, Hannon GJ, et al. 2006. Identification and validation of oncogenes in liver cancer using an integrative oncogenomic approach. *Cell* **125**: 1253–1267.

Zhang J, Xu Z-P, Yang Y-C, Zhu J-S, Zhou Z, Chen W-X. 2012. Expression of Yes-associated protein in gastric adenocarcinoma and inhibitory effects of its knockdown on gastric cancer cell proliferation and metastasis. *Int J Immunopathol Pharmacol* **25**: 583–590.

Zhao B, Kim J, Ye X, Lai ZC, Guan KL. 2009. Both TEAD-Binding and WW Domains Are Required for the Growth Stimulation and Oncogenic Transformation Activity of Yes-Associated Protein. *Cancer Research* **69**: 1089–1098.

Zhao B, Lei Q-Y, Guan K-L. 2008a. The Hippo–YAP pathway: new connections between regulation of organ size and cancer. *Current Opinion in Cell Biology* **20**: 638–646.

Zhao B, Li L, Lei Q, Guan KL. 2010. The Hippo-YAP pathway in organ size control and tumorigenesis: an updated version. *Genes Dev* **24**: 862–874.

Zhao B, Li L, Lu Q, Wang LH, Liu CY, Lei Q, Guan KL. 2011. Angiomotin is a novel Hippo pathway component that inhibits YAP oncoprotein. *Genes Dev* **25**: 51–63.

Zhao B, Ye X, Yu J, Li L, Li W, Li S, Yu J, Lin JD, Wang CY, Chinnaiyan AM, et al. 2008b. TEAD mediates YAP-dependent gene induction and growth control. *Genes Dev* **22**: 1962–1971.

Zhao Z, Ge J, Sun Y, Tian L, Lu J, Liu M, Zhao Y. 2012. Is E-cadherin immunoexpression a prognostic factor for head and neck squamous cell carcinoma (HNSCC)? A systematic review and meta-analysis. *Oral Oncology* **48**: 761–767.

Zhou D, Conrad C, Xia F, Park J-S, Payer B, Yin Y, Lauwers GY, Thasler W, Lee JT, Avruch J, et al. 2009. Mst1 and Mst2 Maintain Hepatocyte Quiescence and Suppress Hepatocellular Carcinoma Development through Inactivation of the Yap1 Oncogene. *Cancer Cell* **16**: 425–438.